

Item	Present?	Filename This should be the name the file is saved as when it is uploaded to our system, and should include the file extension. The extension must be .pdf	A brief, numerical description of file contents. i.e.: <i>Supplementary Figures 1-4, Supplementary Discussion, and Supplementary Tables 1-4.</i>
Supplementary Information	Yes	Supplementary Figures.pdf	Supplementary Figures 1-8
Reporting Summary	Yes	UPDATED Reporting Summary.pdf	

## Genome-wide CRISPR-Cas9 Screening Reveals Ubiquitous T cell Cancer Targeting via the monomorphic MHC class I related protein MR1

Michael D. Crowther<sup>1†</sup>, Garry Dolton<sup>1†</sup>, Mateusz Legut<sup>1</sup>, Marine E. Caillaud<sup>1</sup>, Angharad Lloyd<sup>1</sup>, Meriem Attaf<sup>1</sup>, Sarah A. E. Galloway<sup>1</sup>, Cristina Rius<sup>1</sup>, Colin P. Farrell<sup>2</sup>, Barbara Szomolay<sup>1,3</sup>, Ann Ager<sup>1,3</sup>, Alan L. Parker<sup>4</sup>, Anna Fuller<sup>1</sup>, Marco Donia<sup>5</sup>, James McCluskey<sup>6</sup>, Jamie Rossjohn<sup>1,3,7,8</sup>, Inge Marie Svane<sup>5</sup>, John Phillips<sup>2</sup> and Andrew K. Sewell<sup>1,3\*</sup>

### Affiliations:

<sup>1</sup>Division of Infection and Immunity, Cardiff University School of Medicine, Cardiff, Wales, United Kingdom

<sup>2</sup>Division of Hematology, University of Utah School of Medicine, Salt Lake City, UT, USA

<sup>3</sup>Systems Immunity Research Institute, Cardiff University, Cardiff, Wales, United Kingdom

<sup>4</sup>Division of Cancer and Genetics, Cardiff University School of Medicine, Cardiff, Wales, United Kingdom

<sup>5</sup>Center for Cancer Immune Therapy, Herlev Hospital, Copenhagen University, Copenhagen, Denmark

<sup>6</sup>Department of Microbiology and Immunology, Peter Doherty Institute for Infection and Immunity, University of Melbourne, Parkville, Victoria, Australia

<sup>7</sup>Australian Research Council Centre of Excellence in Advanced Molecular Imaging, Monash University, Clayton, Victoria, Australia

<sup>8</sup>Infection and Immunity Division and Department of Biochemistry and Molecular Biology, Biomedicine Discovery Institute, Monash University, Melbourne, Australia

\*Correspondence to: Professor Andrew Sewell, [sewellak@cardiff.ac.uk](mailto:sewellak@cardiff.ac.uk)

†These authors contributed equally

## **ABSTRACT**

Human Leukocyte Antigen (HLA)-independent, T cell-mediated targeting of cancer cells would allow immune destruction of malignancies in all individuals. Here, we use genome-wide CRISPR-Cas9 screening to establish that a T cell receptor (TCR) recognized and killed most human cancer types via the monomorphic MHC class I related protein, MR1, while remaining inert to non-cancerous cells. Unlike mucosal-associated invariant T (MAIT) cells, recognition of target cells by the TCR was independent of bacterial loading. Furthermore, concentration-dependent addition of

vitamin B-related metabolite ligands of MR1 reduced TCR recognition of cancer cells suggesting that recognition occurred via sensing of the cancer metabolome. An MR1 restricted T cell clone mediated *in vivo* regression of leukemia and conferred enhanced survival of NSG mice. TCR transfer to patient T cells enabled killing of autologous and non-autologous melanoma. These findings offer opportunities for HLA-independent, pan-cancer, pan-population immunotherapies.

## INTRODUCTION

Unconventional T cells do not recognize classical peptide-Major Histocompatibility Complex (pMHC) ligands and can express  $\alpha\beta$  or  $\gamma\delta$  T cell receptors (TCRs). The ligands recognized by many unconventional T cells remain unknown. Established unconventional T cell ligands include lipid antigens presented by the conserved CD1 family of molecules, as recognized by Natural Killer T (NKT) cells and Germline-Encoded Mycolyl-lipid reactive T (GEM) cells. The human V $\gamma$ 9V $\delta$ 2 T cell subset recognizes phosphorylated isoprenoid intermediates of lipid biosynthesis in the context of Butyrophilin 3A1<sup>1</sup>. The concept of T cell sensing of intracellular biosynthetic pathways was recently extended by the discovery that MAIT cells sense microbial metabolites bound to the evolutionarily-conserved, monomorphic MHC-class 1 related protein (MR1)<sup>2,3</sup>. MAIT cell stimulatory antigens have been defined as riboflavin-derived derivatives produced by a range of bacteria and fungi<sup>4</sup>, notably 5-(2-oxopropylideneamino)-6-*D*-ribitylaminouracil (5-OP-RU)<sup>5</sup>. MAITs can rapidly clear pathogens through secretion of a range of cytokines that can be accompanied by granzyme and perforin expression upon recognition of these antigens bound to MR1<sup>6</sup>. MAITs are defined by their semi-invariant TCR gene segment usage consisting of TRAV1-2 rearranged with TRAJ33, 12 or 20, paired with a limited repertoire of TCR- $\beta$  chains<sup>4,7,8</sup>, including but not limited to TRBV6 and TRBV20. More recent evidence shows that recognition of MR1-associated ligands can be accomplished by a wider range of

58 TCR rearrangements including those using TRAV14, TRAV21 and TRAV36 chains and that MR1 can present a broader range of ligands than those  
59 from the riboflavin biosynthetic pathway, incorporating diverse chemical scaffolds which includes drugs and drug-like molecules<sup>9-13</sup>. In  
60 combination, these data suggest that MR1 presents a wide range of metabolic intermediates at the cell surface in much the same way as MHC  
61 molecules present arrays of peptides, and the CD1 family of molecules present various lipid antigens. T cell targeting of diseases via MHC Ib and  
62 MHC-I like molecules such as CD1 and MR1 is especially attractive as, unlike the highly polymorphic human leukocyte antigen (HLA) targets of  
63 conventional T cells, these molecules are largely monomorphic in the human population. Indeed, MR1 is ubiquitously expressed and the  
64 currently known non-peptide ligands it presents cannot mutate as they are essential biosynthetic intermediates to many microbes<sup>14</sup>. While most  
65 studies have indicated MR1 is only expressed on the cell surface after an MR1-binding ligand has bound<sup>14,15</sup> there is evidence that there is a basal  
66 surface expression, including on cancer cells<sup>9,16</sup>. Intratumoural unconventional T cell infiltrations have also been associated with favorable  
67 prognostic outcome<sup>17</sup>, with MAIT cells also shown to have a role in multiple myeloma<sup>18</sup>. Human MR1 has a very limited number of silent and  
68 intronic polymorphisms<sup>19,20</sup> and natural isoforms<sup>21</sup>, highlighting its potential as a pan-population target. Currently, there are no self-ligands  
69 identified that bind to MR1 that induce a T cell response. However, there is increasing evidence that populations of MR1-restricted cells exist  
70 that likely respond to self-antigens<sup>9,16</sup>. These MR1-restricted T cells are not classical MAIT cells in that they do not appear to possess a TRAV1-2  
71 TCR nor do they react to bacterial antigens bound to MR1. Here we report of a novel non-MAIT TCR that recognizes a non-bacterial antigen  
72 restricted by MR1 resulting in lysis of cancer cells. This TCR does not respond to healthy cells but confers HLA-independent recognition to a wide  
73 range of cancer cells.

74



## RESULTS

### Clone MC.7.G5 kills a broad range of cancer cells regardless of HLA allomorph

A T cell population that proliferated in response A549 cancer cells was grown from the peripheral blood mononuclear cells from an HLA-mismatched healthy donor (**Fig. 1a**). Recognition of A549 cells by the  $\alpha\beta\text{TCR}^+ \gamma\delta\text{TCR}^{\text{neg}} \text{CD8}\alpha^+ \text{CD8}\beta^{\text{low}} \text{CD4}^{\text{neg}}$  (**Supplementary Fig. 1a**) T cell clone MC.7.G5 grown from this line was not reduced by blocking MHC antibodies (**Fig. 1b**). TCR sequencing of MC.7.G5 confirmed expression of an  $\alpha\beta\text{TCR}$ ; comprised of a TRAV38.2/DV8 TRAJ31  $\alpha$ -chain paired with a TRBV25.1 TRBJ2.3  $\beta$ -chain (**Supplementary Fig. 1b**). MC.7.G5 killed multiple cancer cell lines tested (lung, melanoma, leukemia, colon, breast, prostate, bone and ovarian) that did not share a common HLA (**Fig. 1c**). MC.7.G5 also killed minimally-cultured primary ovarian and melanoma cancer cells, indicating that killing was not an artifact of long-term culture (**Fig. 1c**). MC.7.G5 remained inert to healthy cells (**Fig. 1d**) and showed high sensitivity to a melanoma target at low effector to target ratios (**Fig. 1e**). As MC.7.G5 preferentially killed cancer cells independently of classical MHC molecules we set-out to uncover its mechanism of action.

### Genome-wide CRISPR-Cas9 screening revealed MR1 as the MC.7.G5 target on cancer cells

As MC.7.G5 killed a wide range of cancer cell lines originating from different tissues and organs regardless of their HLA allomorph expression, its mode of target cell recognition was unclear. A genome-wide CRISPR-Cas9 approach, using the GeCKOv.2 library<sup>22,23</sup> which targets every protein-coding gene in the human genome with six different single guide (sg)RNAs, was used to identify genes essential for recognition of target cells by MC.7.G5 (**Fig. 2a**). Following two rounds of selection with MC.7.G5 the surviving transduced HEK293T cells exhibited reduced capacity to stimulate MC.7.G5, suggesting key genes involved in their recognition had been ablated (**Fig. 2b**). Sequencing of the CRISPR sgRNAs in the lysis-

resistant HEK293T cells showed that only 6 genes were targeted by more than one enriched sgRNA:  $\beta$ 2M (five sgRNAs), MR1 (two sgRNAs), regulatory factor X (RFX, five sgRNAs), RFX associated ankyrin containing protein (RFXANK, five sgRNAs), RFX associated protein (RFXAP, three sgRNAs), and signal transducer and activator of transcription 6 (STAT6, two sgRNAs) (**Fig. 2c**). RFX, RFXANK and RFXAP are essential components of the protein complex responsible for transactivating  $\beta$ 2M, MHCI and MHCII promoters<sup>24</sup>. Combined with the fact that  $\beta$ 2M and MR1 heterodimerise to form a monomorphic stable antigen-presenting molecule known to activate MAITs and other MR1-restricted T cells, these data strongly suggested that the MC.7.G5 T cell recognized cancer targets via the MR1 molecule. Accordingly, anti-MR1 antibody, but not MHCI or MHCII antibodies, blocked target cell recognition by MC.7.G5 (**Fig. 3a**). CRISPR-mediated knockout of MR1 from A549<sup>11</sup> and melanoma MM909.24 (frame-shift deletion mutation shown in **Supplementary Fig. 2a**) protected against MC.7.G5-mediated recognition and lysis (**Fig. 3b**). Melanoma MM909.24 did not stain with anti-MR1 antibody suggesting that very minimal levels of MR1 were required for target recognition (**Supplementary Fig. 2b**). Overexpression of MR1 resulted in strong recognition of the poorly recognized targets, HeLa and C1R (MR1 staining in **Supplementary Fig. 2b**), and slightly enhanced recognition of melanoma MM909.24 (**Fig. 3c**). Reintroduction of MR1 in to CRISPR-Cas9 MR1-knockout A549 cells under a CMV promoter<sup>11</sup> restored recognition by MC.7.G5 (**Fig. 3d**), instilling further confidence that cancer cell recognition was MR1-dependent. In summary, whole genome CRISPR screening effectively revealed MR1 as the restricting molecule on cancer cells for the HLA-agnostic T cell clone MC.7.G5.

#### **MC.7.G5 does not recognise MR1 by known mechanisms**

108 MR1 is known to present intermediates in riboflavin synthesis at the cell surface to MAIT cells and is not considered to be expressed appreciably  
109 at the cell surface without a bound cargo<sup>14</sup>. MC.7.G5 did not stain with tetramers composed of MR1 containing the K43A mutation that allows  
110 MR1 refolding without bound ligand (**Fig. 4a**)<sup>13</sup>. Accordingly, MC.7.G5 did not recognize C1R cells transduced with the MR1 K43A mutant (**Fig. 4b**)  
111 despite high overexpression of surface MR1 K43A detectable by anti-MR1 antibody staining (**Supplementary Fig. 2b**). This demarcates MC.7.G5's  
112 recognition of target cells from the previously described 'MR1T' cells that do not require K43 for activation<sup>9</sup>. The requirement for the ligand-  
113 binding K43 suggested that MC.7.G5 might recognize an MR1-bound ligand that was specifically expressed or upregulated in malignant cells. In  
114 concordance with this hypothesis, MC.7.G5 did not stain with tetramers assembled with MR1 presenting microbial derived T cell activator 5-OP-  
115 RU (**Fig. 4a**). Furthermore, recognition of target cells was reduced when loaded with either the MAIT activating bacterium *Mycobacterium*  
116 *smegmatis* (*M. smeg*) or *Salmonella enterica* serovar Typhimurium (**Fig. 4c&d**), or MR1 ligand Acetyl-6-Formylpterin (Ac-6-FP)<sup>11,25</sup> (**Fig. 4e**),  
117 despite a slight increase in surface expression of MR1 (**Supplementary Fig. 2c**). MC.7.G5 exhibited cancer specificity unlike the majority of MR1T  
118 cells<sup>9</sup>, which require over-expression of MR1 for optimal target cell recognition and also activated in response to MR1 expression by healthy  
119 monocyte derived dendritic cells. MC.7.G5 did not recognize immature or matured monocyte derived dendritic cells (**Fig. 5a**), nor Langerhans  
120 cells (**Fig. 5b**). These results indicate that MC.7.G5 does not exclusively recognize MR1 *per se*, nor MR1 by known mechanisms, but rather MR1  
121 with bound cargo that is specific to, or associated with, cancer cells. A MC.7.G5-like T cell clone was grown from a second donor, which was also  
122 dependent on K43 for target cell recognition (**Supplementary Fig. 3**), suggesting that cancer-specific T cells capable of recognizing wild-type  
123 levels of MR1 may be present in multiple individuals.

124

### MC.7.G5 remained inert to resting, activated, stressed or infected healthy cells from various tissues

In order to assess the safety of using the MC.7.G5 TCR for cancer immunotherapy we undertook further testing of healthy cells from various tissues. In extension to the data shown in **Fig. 1** (smooth muscle, lung fibroblast and liver cells) and **Fig. 5a&b** (dendritic and Langerhans cells), MC.7.G5 did not kill healthy cells from lung (alveolar and bronchus), skin (melanocytes), intestine, pancreas or kidney (**Fig. 5c**). In the same assay >95% of each cancer cell line from lung, skin (melanomas), blood, cervix and kidney were killed, whereas cancer cell lines rendered negative for MR1 using CRISPR-Cas9 were not killed (**Fig. 5c**). Next, we created conditions that may induce cellular upregulation of cell surface MR1, or generate ligands bound to MR1. T or B cells sorted directly *ex vivo* and activated overnight with either PHA or TLR9 ligand respectively (CD69 staining, **Supplementary Fig. 4a**) were untouched by MC.7.G5 (**Fig. 6a**). Lymphoblastoid cell lines that are relatively poor targets of MC.7.G5, did not activate MC.7.G5 following treatment with *tert*-Butyl hydroperoxide (tBHP) (**Fig. 6b**) to induce cell stress (ROS detection, **Supplementary Fig. 4b**). Furthermore, a normal renal epithelial cell line did not become targets when treated with tBHP or H<sub>2</sub>O<sub>2</sub> (ROS detection, **Supplementary Fig. 4b**), which induce different pathways of cell stress<sup>26</sup>, or by exposure to  $\gamma$ -irradiation (**Fig. 6b**). *M. smeg* infection of healthy lung epithelial cells did not lead to MC.7.G5 activation, whereas the infected cells were recognized by a MAIT T cell line (**Fig. 6c**). Therefore, healthy cells are incapable of activating MC.7.G5, even when stressed or damaged.

### MC.7.G5 controls leukemia in vivo

To examine the *in vivo* capacity of MC.7.G5 to target cancer, Jurkat leukemia cells were engrafted in NSG mice followed by the adoptive transfer of MC.7.G5. Bone marrow samples were analyzed for MC.7.G5 and Jurkat cell frequencies at days 12 and 18 post T cell transfer. MC.7.G5

appeared in the bone marrow at both time points but the number of cells remaining on day 18 following the single transfusion was substantially reduced (**Fig. 7a**). Mice receiving MC.7.G5 had significantly less Jurkat cells at days 12 and 18 (**Fig. 7a**) than mice with no MC.7.G5. The difference in Jurkat cell burden was particularly striking at day 18 with mice receiving MC.7.G5 having 3.8%, 7.2% and 0.3% Jurkat cells in the bone marrow, compared to 83%, 78% and 85% for the mice without MC.7.G5 (**Fig. 7a**). The presence of Jurkat cells was also reduced in the spleen of mice that received T cells, with a similar drop in T cell numbers by day 18 (**Supplementary Fig. 5**). The *in vivo* targeting of Jurkat cells by MC.7.G5 was dependent on MR1 expression, as shown by co-transfer experiments with differentially labelled Jurkat wild-type and Jurkat *MR1*<sup>-/-</sup> cells to the same mice (**Fig. 7b**). The ability of MC.7.G5 to target Jurkat cells *in vivo* translated to a significant enhancement of survival for mice that received T cells (**Fig. 7c**). These data demonstrate that MC.7.G5 maintained its reactivity towards cancer cells in an *in vivo* setting thus reducing cancer burden and enhancing survival.

#### **The MC.7.G5 redirects patient T cells to kill autologous cancer cells**

To explore the therapeutic potential of targeting MR1 on cancer cells we purified T cells from the PBMCs of Stage IV melanoma patients and lentivirally transduced them with the MC.7.G5 TCR (≥85% expression, **Supplementary Fig. 6a**), which resulted in recognition and killing of autologous and non-autologous melanomas (**Fig. 8a&b**), but not healthy cells (**Fig. 8b**). The killing was specific to MR1 as the MC.7.G5 TCR transduced cells did not lyse MR1 knockout melanomas (**Fig. 8b**). We conclude that the MC.7.G5 TCR can redirect patient T cells to kill patient cancer cells without the requirement of a specific HLA.

## DISCUSSION

MR1 is an attractive target for cancer immunotherapy due to its monomorphic, ubiquitously-expressed nature. Recent advances in MR1 tetramers and ligand discoveries have progressed knowledge in this area but there is still much to be discovered. Here we confirmed cancer cell recognition by a T cell clone that responded to multiple cancer cell lines from diverse tissue types, resulting in killing of cancer cells *in vitro* and *in vivo*. The clone expresses a TCR that is not indicative of MAIT cells. Current MR1 antibodies are unable to detect low surface expression of MR1 on cancer cells, despite detectable mRNA expression<sup>15</sup>. Indeed, the level of MR1 surface expression required for cancer cell recognition by MC.7.G5 was often below the threshold required for staining with antibody, suggesting that the MC.7.G5 TCR might be capable of responding to a low copy number of MR1 ligand, akin to T cells that recognize pMHC and MAIT TCR recognition of MR1<sup>27</sup>. Our results also demonstrate the immense power of genome-wide CRISPR-Cas9 screening as a discovery platform for unconventional T cell ligands and we anticipate that the methodologies applied here will rapidly revolutionize the unconventional T cell field by revealing new ligands. Further work will be required to establish the exact nature of the ligand recognized by the MC.7.G5 TCR. Knowledge of known MR1-restricted ligands suggests that the MC.7.G5 TCR ligand may be a cancer-specific or -associated metabolite. We failed to find hits in a metabolic pathway during our genome-wide CRISPR-Cas9 screens. This suggests that the MR1-associated ligand targeted by the MC.7.G5 TCR is part of a pathway essential for the basic survival of cancer cells and therefore not amenable for the gene disruption required for CRISPR-Cas9 screening.

In summary, we describe a TCR that exhibits pan-cancer cell recognition via the invariant MR1 molecule, and by equipping melanoma patient T cells that lacked detectable cancer cell reactivity with the MC.7.G5 TCR, rendered them capable of killing autologous melanoma. Importantly,

178 MC.7.G5 did not respond to healthy cells and caused no obvious pathology in the healthy donor it was grown from. Since the MC.7.G5 TCR can  
179 recognize diverse cancer cell type, including primary cancer cells, irrespective of HLA it opens up exciting opportunities for pan-cancer, pan-  
180 population T cell-mediated cancer immunotherapy approaches. Discovery of the MR1-restricted ligands recognized by MC.7.G5-like T cells may  
181 further open up opportunities for therapeutic vaccination for many cancers in all individuals.

182

### 183 **ACKNOWLEDGEMENTS**

184 Thanks to F. Zhang for deposition of the GeCKOv.2 library at the Addgene plasmid repository (Addgene plasmid #1000000048); D. Trono for the  
185 deposition of pRRL.sin.cppt.pgk-gfp.wpre (Addgene plasmid #12252), envelope plasmid pMD2.G (Addgene plasmid #12259), and packaging  
186 plasmids pMDLg/pRRE (Addgene plasmid #12251) and pRSV-Rev (Addgene plasmid #12253); and J. Riley, University of Pennsylvania, PA, who  
187 kindly provided the pELNS vector. AKS is a Wellcome Senior Investigator (WT100327MA), MDC was funded by the Welsh Assembly Government  
188 via a Health and Care Research Wales PhD studentship. ML is funded by a Consolidator Award via the Wellcome Institutional Strategic Support  
189 Fund to the Cardiff University College of Biomedical and Life Sciences.

190

### 191 **AUTHOR CONTRIBUTIONS**

192 AKS and GD conceived project. MDC, GD, MEC, SAEG, MA, AL and CR undertook the T cell experiments; MDC, ML, CPF, BS and JP performed the  
193 genome-wide CRISPR experiments and/or analyses; AF generated lentiviral vectors and edited the manuscript; MD and IMS supplied the patient  
194 PBMC and melanoma and renal carcinoma cell lines; AA provided advice on mouse experiments; ALP provided expertise and ovarian cancer  
195 ascites; JR and JMc provided the MR1 tetramer reagents; GD and AKS supervised the work; MDC, GD and AKS wrote and edited the manuscript.

196

### 197 **COMPETING INTERESTS**

198 Cardiff University has filed patents based on these findings.

## REFERENCES

1. Vavassori, S. *et al.* Butyrophilin 3A1 binds phosphorylated antigens and stimulates human  $\gamma\delta$  T cells. *Nat. Immunol.* **14**, 908–916 (2013).
2. Kjer-Nielsen, L. *et al.* MR1 presents microbial vitamin B metabolites to MAIT cells. *Nature* **491**, 717–723 (2012).
3. Corbett, A. J. *et al.* T-cell activation by transitory neo-antigens derived from distinct microbial pathways. *Nature* **509**, 361–5 (2014).
4. Gold, M. C. *et al.* MR1-restricted MAIT cells display ligand discrimination and pathogen selectivity through distinct T cell receptor usage. *J. Exp. Med.* **211**, 1601–1610 (2014).
5. Eckle, S. B. G. *et al.* Recognition of Vitamin B precursors and byproducts by mucosal associated invariant T cells. *J. Biol. Chem.* **290**, 30204–30211 (2015).
6. Le Bourhis, L. *et al.* Antimicrobial activity of mucosal-associated invariant T cells. *Nat. Immunol.* **11**, 701–708 (2010).
7. Reantragoon, R. *et al.* Structural insight into MR1-mediated recognition of the mucosal associated invariant T cell receptor. *J. Exp. Med.* **209**, 761–774 (2012).
8. Lepore, M. *et al.* Parallel T-cell cloning and deep sequencing of human MAIT cells reveal stable oligoclonal TCR $\beta$  2 repertoire. *Nat. Commun.* **5**, 3866 (2014).
9. Lepore, M. *et al.* Functionally diverse human T cells recognize non-microbial antigens presented by MR1. *Elife* **6**, 1–22 (2017).
10. Gherardin, N. A. *et al.* Diversity of T Cells Restricted by the MHC Class I-Related Molecule MR1 Facilitates Differential Antigen Recognition. *Immunity* **44**, 32–45 (2016).
11. Laugel, B. *et al.* Engineering of Isogenic Cells Deficient for MR1 with a CRISPR/Cas9 Lentiviral System: Tools To Study Microbial Antigen Processing and Presentation to Human MR1-Restricted T Cells. *J. Immunol.* **197**, 971–982 (2016).
12. Keller, A. N. *et al.* Drugs and drug-like molecules can modulate the function of mucosal-associated invariant T cells. *Nat. Immunol.* (2017). doi:10.1038/ni.3679
13. Reantragoon, R. *et al.* Antigen-loaded MR1 tetramers define T cell receptor heterogeneity in mucosal-associated invariant T cells. *J. Exp. Med.* **210**, 2305–20 (2013).
14. McWilliam, H. E. G. *et al.* The intracellular pathway for the presentation of vitamin B–related antigens by the antigen-presenting molecule MR1. *Nat. Immunol.* **advance on**, 1–9 (2016).
15. Lamichhane R and Ussher JE. Expression and trafficking of MHC related protein 1 (MR1). *J. Immunol.* **38**, 42–49 (2017).
16. Young, M. H. *et al.* MAIT Cell Recognition of MR1 on Bacterially Infected and Uninfected Cells. *PLoS One* **8**, e53789 (2013).
17. Gentles, A. J. *et al.* The prognostic landscape of genes and infiltrating immune cells across human cancers. *Nat. Med.* **21**, 938–945 (2015).
18. Gherardin, N. A. *et al.* Enumeration, functional responses and cytotoxic capacity of MAIT cells in newly diagnosed and relapsed multiple myeloma. *Sci. Rep.* **8**, 4159 (2018).
19. Parra-Cuadrado, J. F. *et al.* A study on the polymorphism of human MHC class I-related MR1 gene and identification of an MR1-like pseudogene. *Tissue Antigens* **56**, 170–2 (2000).
20. Seshadri, C. *et al.* A polymorphism in human MR1 is associated with mRNA expression and susceptibility to tuberculosis. *Nat. Publ. Gr.* **18**,



8–14 (2016).

21. Lion, J. *et al.* MR1B , a natural spliced isoform of the MHC-related 1 protein , is expressed as homodimers at the cell surface and activates MAIT cells. 1363–1373 (2013). doi:10.1002/eji.201242461
22. Shalem, O. *et al.* Genome-scale CRISPR-Cas9 knockout screening in human cells - supplement. *Science (80-. ).* **343**, 84–87 (2014).
23. Patel, S. J. *et al.* Identification of essential genes for cancer immunotherapy. *Nature* **548**, 537–542 (2017).
24. Reith, W., LeibundGut-Landmann, S. & Waldburger, J.-M. Regulation of MHC class II gene expression by the class II transactivator. *Nat. Rev. Immunol.* **5**, 793–806 (2005).
25. Eckle, S. B. G. *et al.* A molecular basis underpinning the T cell receptor heterogeneity of mucosal-associated invariant T cells. *J. Exp. Med.* **211**, 1585–1600 (2014).
26. Alía, M., Ramos, S., Mateos, R., Bravo, L. & Goya, L. Response of the antioxidant defense system to tert-butyl hydroperoxide and hydrogen peroxide in a human hepatoma cell line (HepG2). *J. Biochem. Mol. Toxicol.* **19**, 119–128 (2005).
27. Irvine, D. J., Purbhoo, M. A., Krogsgaard, M. & Davis, M. M. Direct observation of ligand recognition by T cells. *Nature* **419**, 845–849 (2002).
28. Hulin-Curtis, S. L. *et al.* Histone deacetylase inhibitor trichostatin A sensitises cisplatin-resistant ovarian cancer cells to oncolytic adenovirus. *Oncotarget* **9**, 26328–26341 (2018).
29. Wooldridge, L. *et al.* MHC Class I Molecules with Superenhanced CD8 Binding Properties Bypass the Requirement for Cognate TCR Recognition and Nonspecifically Activate CTLs. *J. Immunol.* **184**, 3357–3366 (2010).
30. Lissina, A. *et al.* Protein kinase inhibitors substantially improve the physical detection of T-cells with peptide-MHC tetramers. *J. Immunol. Methods* **340**, 11–24 (2009).
31. Tungatt, K. *et al.* Antibody Stabilization of Peptide-MHC Multimers Reveals Functional T Cells Bearing Extremely Low-Affinity TCRs. *J. Immunol.* **194**, 463–474 (2014).
32. Betts, M. R. *et al.* Sensitive and viable identification of antigen-specific CD8+ T cells by a flow cytometric assay for degranulation. *J. Immunol. Methods* **281**, 65–78 (2003).
33. Haney, D. *et al.* Isolation of viable antigen-specific CD8+ T cells based on membrane-bound tumor necrosis factor (TNF)- $\alpha$  expression. *J. Immunol. Methods* **369**, 33–41 (2011).
34. Shalem, O. *et al.* Genome-scale CRISPR-Cas9 knockout screening in human cells. *Science (80-. ).* **343**, 84–87 (2014).
35. Ryan, M. D., King, A. M. Q. & Thomas, G. P. Cleavage of foot-and-mouth disease virus polyprotein is mediated by residues located within a 19 amino acid sequence. *J. Gen. Virol.* **72**, 2727–2732 (1991).
36. Sanjana, N. E., Shalem, O. & Zhang, F. Improved vectors and genome-wide libraries for CRISPR screening. *Nat. Methods* **11**, 783–784 (2014).
37. Li, W. *et al.* MAGeCK enables robust identification of essential genes from genome-scale CRISPR/Cas9 knockout screens. *Genome Biol.* **15**, 554 (2014).
38. Maciocia, P. M. *et al.* Targeting the T cell receptor  $\beta$ -chain constant region for immunotherapy of T cell malignancies. *Nat. Med.* (2017). doi:10.1038/nm.4444

## Legends

**Figure 1: MC.7.G5 recognises multiple cancer types through an HLA-independent mechanism.** (a) MC.7.G5 was cloned from T cells that proliferated in response to cancer cell line A549. Performed once for this donor. (b) MC.7.G5 did not recognise A549 through MHCI or MHCII. Overnight activation +/- blocking antibodies and TNF ELISA. Bars depict the mean. (c) MC.7.G5 killed a range of established (long-term culture) and primary cancer cell lines of different origin. Flow-based killing assay for 48-72h at a T cell to target cell ratio of 5:1. Data combined from different experiments. Performed in triplicate. (d) MC.7.G5 killed melanoma cells but not healthy cells. Flow based killing assay at a T cell to target cell ratio of 5:1. Performed in triplicate or duplicate (fibroblasts). (e) MC.7.G5 sensitively killed melanoma MM909.24 over 7 days. Performed in duplicate. **b-e** Bars, horizontal lines and connecting line depict the mean.

**Figure 2: Whole genome CRISPR-Cas9 library screening reveals MR1 as the candidate target of MC.7.G5.** (a) Overview of the approach used to reveal the ligand of MC.7.G5. GeCKO v2 whole genome CRISPR-Cas9 libraries A and B were used as lentivirus to transduce target cell line HEK293T. MC.7.G5 lysed HEK293T expressing sgRNAs for genes that are irrelevant for HEK293T recognition, thereby enriching sgRNAs for genes that are essential for cancer cell lysis by MC.7.G5. Two rounds of selection with MC.7.G5 were performed and comparison of selected libraries unselected HEK293T (no MC.7.G5) revealed enriched sgRNAs. (b) MC.7.G5 recognition of selected HEK293T library post-selection is greatly reduced compared to wild-type HEK293T, suggesting key genes had been ablated by the whole genome CRISPR-Cas9 approach. Overnight activation and TNF ELISA, performed in duplicate. Bars depict the mean. (c) MR1 was identified as one of key genes for MC.7.G5 recognition of

285 HEK293T. Total genomic DNA from  $3 \times 10^7$  selected and unselected HEK293T libraries was used for sequencing, followed by MAGeCK analysis.  
286 Highlighted (coloured) genes with y genes for MC.7.G5 recognition of HEK293T.reduced

287  
288 **Figure 3. MR1 is the cancer cell expressed target of MC.7.G5.** (a) Recognition of melanoma MM909.24 was reduced in the presence of MR1  
289 blocking antibody (Ab). MHCI and II Abs were used as negative controls. Overnight activation and TNF ELISA. (b) Removal of MR1 expression  
290 (CRISPR/Cas9) from cancer cell lines prevented MC.7.G5 mediated recognition and killing. Overnight activation and TNF ELISA or chromium  
291 release cytotoxicity assay. (c) Lentiviral overexpression (+) of MR1 in poor targets of MC.7.G5 improved target cell killing by MC.7.G5. Chromium  
292 release cytotoxicity assay. (d) Lentiviral expression of MR1 in *MR1*<sup>-/-</sup> cells restores activation of MC.7.G5. TNF ELISA. Conditions performed in  
293 duplicate. Bars depict the mean.

294  
295 **Figure 4. MC.7.G5 does not recognise MR1 by known mechanisms.** (a) MC.7.G5 did not stain with empty (K43A) or MR1 5-OP-RU tetramers. A  
296 canonical MAIT clone recognizes MR1 bound with 5-OP-RU. The MHCI-restricted clone was used as a positive control for the irrelevant MHCI  
297 tetramer. Performed twice with similar results. (b) MC.7.G5 recognised target cells over-expressing wildtype MR1 (*MR1*<sup>++</sup>) but not K43A mutated  
298 MR1. Overnight activation performed in duplicate and TNF ELISA. (c) Loading with MAIT-activating bacterium *Mycobacterium smegmatis*  
299 (*M.smeg*) reduced MC.7.G5 recognition of A549 cells. Canonical MAIT clone used as a positive control. Staining for surface CD107a and  
300 intracellular TNF. Performed twice with similar results. (d) *M. smeg* and *Salmonella enterica* serovar Typhimurium (S.Typhimurium) reduced  
301 MC.7.G5 recognition of A549 cells. Overnight activation and TNF ELISA. (e) Exogenous Ac-6-FP, a known MR1 binding molecule, reduced

302 MC.7.G5 recognition of melanoma MM909.24. Percentage of cell triple positive for the markers shown is plotted. Performed twice with similar  
303 results.

304

305 **Figure 5. MC.7.G5 does not recognise healthy cells.** (a) MC.7.G5 did not recognize immature or matured monocyte (mo) derived dendritic cells  
306 (DCs). Overnight activation and TNF ELISA. (b) MC.7.G5 did not recognize matured Langerhans cells. CD1a-restricted clone 40E.22 used as a  
307 positive control for recognition of Langerhans cells. Overnight activation and TNF ELISA. (c) Cancer cell lines lacking MR1 (CRISPR/Cas9) and  
308 healthy cells from various tissues were not killed by MC.7.G5. Flow-based killing assay (48h 1:1 ratio). Performed in triplicate. **a-c** bars depict the  
309 mean.

310

311 **Figure 6. MC.7.G5 remained inert to activated, stressed or infected healthy cells.** (a) T cell (Jurkat) and B cell (K562) cancer cells were targets of  
312 MC.7.G5, whereas whole PBMCs and resting or activated purified T and B cells were not killed. Flow-based killing assay (24h 1:1 ratio).  
313 Performed in triplicate. (b) Experiment 1: tert-Butyl hydroperoxide (tBHP) treatment to induce stress in poor targets (C1R and SAR26  
314 lymphoblastoid cell lines) of MC.7.G5 did not lead to T cell activation. MC.7.G5 recognition of melanoma MM909.24 +/- MR1 was unaffected by  
315 tBHP treatment. Experiment 2: Healthy renal epithelial cells were not recognised by MC.7.G5 following treatment with either tBHP or hydrogen  
316 peroxide (H<sub>2</sub>O<sub>2</sub>), or after exposure to  $\gamma$ -irradiation. Overnight activation and TNF ELISA. Inserted histogram of irradiated renal cells stained with  
317 the viability dye VIVID showing cell death after irradiation compared to un-irradiated cells. (c) *Mycobacterium smegmatis* infected healthy lung  
318 epithelial cells did not lead to MC.7.G5 activation, whereas a MAIT line recognised the infected cells. Uninfected or infected A459 cells +/- MR1

319 acted as controls for MC.7.G5 and the MAIT line respectively. The MAIT line exhibited some recognition towards the uninfected lung cells. TAPI-0  
320 assay for 4h. Percentage shown for duplicate conditions. Performed twice with similar results. **a-c** bars depict the mean.

321

322 **Figure 7. MC.7.G5 mediates *in vivo* regression of leukemia and prolongs the survival of mice.** (a) NSG mice received Jurkat cells ( $3 \times 10^6$ ) then a  
323 single infusion of MC.7.G5 ( $1.5 \times 10^6$ ) 7 days later. MC.7.G5 reduced Jurkat cells in bone marrow cells at day 12 (n=10) and 18 (n=6) post T cell  
324 transfer (left axis). P values (\* 0.032 \*\* 0.0038) from a two-sided non-parametric two-sample Kolmogorov-Smirnov test. Horizontal line depicts  
325 mean and error bars the SD. Jurkat cells did not appear in the spleen at day 12 but MC.7.G5 reduced Jurkat cell load by day 18. Few MC.7.G5  
326 cells were recovered from the bone marrow 18 days after single infusion (right y-axis), and also from the spleen. (b) WT MR1 expressing Jurkat  
327 cells were preferentially targeted in mice receiving MC.7.G5. The same number of MR1 WT and  $MR1^{-/-}$  (DsRed-Express2+) Jurkat cells ( $4 \times 10^6$  in  
328 total) were co-transferred to the same mouse (n=7 per group) followed 7 days later by  $3 \times 10^6$  MC.7.G5. Splenocytes were harvested on day d25  
329 post T cell transfer. (c) Enhanced survival of mice with Jurkat cancer that received MC.7.G5. 8 mice per group (+/- T cells). Experimental set-up as  
330 in (a). Mice were culled when they had lost 15% of their original body weight as required by UK Home Office rules. Median survival of 60.5 and  
331 30.5 days for +/- T cells respectively. Logrank two-sided p value (\*\*\*\* 0.000066) and Hazard Ratio (4.54, 1.27-16.21) were calculated using the  
332 MatSurv survival analysis function in Matlab, available at <https://www.github.com/aebergi/MatSurv>.

333

334 **Figure 8. Transfer of the MC.7.G5 T cell receptor redirects patient T cells to recognise autologous melanoma.** (a) Metastatic melanoma patient  
335 (MM909.11 and MM909.24) derived T cells transduced with the T cell receptor of MC.7.G5 recognised autologous and non-autologous

336 melanomas. Surface CD107a and intracellular TNF after 4h. Performed twice with similar results. (b) T cells from patient MM909.11 transduced  
337 with MC.7.G5 TCR killed autologous and non-autologous melanomas, but not healthy cells. Flow-based killing assay for 36h at a T cell to target  
338 cell ratio of 5:1. Bars depict the mean.

339  
340

## 341 **Methods**

### 342 *Patient and human tissue*

343 Stage IV metastatic melanoma patients MM909.11 and MM909.24 underwent rapid tumor infiltrating therapy for at the Centre for Cancer  
344 Immunotherapy (CCIT), Herlev Hospital, Copenhagen (ethics reference EudraCT no. 2008-008141-20). Ovarian cancer ascites was sourced  
345 through the Wales Cancer Bank (ethics reference WCB14/004) from a stage 3 chemotherapy resistant patient (50001389) at Velindre Cancer  
346 Centre (Cardiff, United Kingdom). Blood was sourced from the Welsh Blood Service (Pontyclun, United Kingdom). The use of human blood was  
347 approved by the School of Medicine Research Ethics Committee (reference 18/56). All human blood was procured and handled in accordance  
348 with the guidelines of Cardiff University to conform to the United Kingdom Human Tissue Act 2004. All samples were taken with informed  
349 consent from participants.

350

### 351 *Cell lines*

352 Cell lines were regularly tested for mycoplasma, and cultured based on ATCC guidelines; breast adenocarcinomas MCF-7 (HTB-22™); prostate  
353 adenocarcinoma LnCAP (CRL-1740™); cervical adenocarcinomas HeLa (CCL-2™) and SiHa (HTB-36™); acute lymphoblastic leukaemia MOLT3

354 (CRL-1552<sup>TM</sup>); chronic myeloid leukaemia K562 (CRL-3344<sup>TM</sup>); myeloma/plasmacytoma U266 (TIB-196<sup>TM</sup>); osteosarcoma U-2 OS (HTB-96<sup>TM</sup>);  
355 immortalized embryonic kidney cell HEK293T (CRL-1573<sup>TM</sup>); acute monocytic leukaemia THP-1 (TIB-202<sup>TM</sup>); lung carcinoma A549 (CCL-185<sup>TM</sup>);  
356 acute T cell leukaemia Jurkat (TIB-152<sup>TM</sup>); colorectal adenocarcinoma COLO 205 (CCL-222<sup>TM</sup>); and ovarian carcinoma A2780 (ECACC 93112519 for  
357 culture guidelines). Melanomas FM-45, MM909.11 and MM909.24, and renal cell carcinoma RCC17 were sourced from the CCIT, and MEL 624  
358 from in-house, with all being cultured in R10 (RPMI 1640 supplemented with 10% foetal bovine serum (FBS), 100 U/mL penicillin, 100 µg/mL  
359 streptomycin and 2 mM L-Glutamine (Life Technologies, Paisely, UK) at 37°C as adherent monolayers, passaged when 50-80% confluent using 2  
360 mM EDTA D-PBS to detach cells. C1R and lymphoblastoid cell line (LCL) SAR26 were sourced or generated in-house and cultured in R10 as  
361 suspension cells. The primary epithelial ovarian cancer cell line EOC031 was generated from ascites following previous guidelines<sup>28</sup> with the  
362 following amendments: the ascites was diluted 1:10 with R10 and centrifuged to collect the cells, which were subsequently depleted of red  
363 blood cells and debris using standard density gradient centrifugation. DMEM-F12 media (Life Technologies) was supplemented as for R10 with  
364 the addition of 5% human serum. Once cells had attached to the flasks and grown for 3 days fibroblasts were removed by incubation with  
365 Trypsin/EDTA for 1 min leaving the ovarian cancer cells for assays. Primary melanomas lines MM909.11, MM909.20 and MM909.21 were  
366 sourced from the CCIT and used directly from cryopreserved samples for killing assays without prior culture. Normal/healthy cells and their  
367 proprietary culture media were obtained from ScienCell (Carlsbad, CA, USA): SMC3 (colonic smooth muscle); CIL-1 (non-pigmented bronchial  
368 ciliary epithelium); HH (hepatocyte); pulmonary alveolar epithelia; melanocytes; renal epithelia; and pancreatic stellate cells. MRC5s (fibroblast)  
369 were sourced locally and cultured as described by the ATCC. Intestinal epithelia and their media were sourced from Lonza (Basel, Switzerland).  
370 Dendritic cells and Langerhans were generated from CD14<sup>+</sup> cells purified from PBMCs using magnetic beads (Miltenyi Biotec Ltd, Bisley, UK).

371 Briefly, both immature DCs and LCs were differentiated with GM-CSF (20 ng/mL) and IL-4 (10 ng/mL), sourced from Miltenyi Biotec Ltd, with LCs  
372 also receiving 20 ng/mL of TGF $\beta$  (Miltenyi Biotec Ltd), for 7-10 days before maturation for 48h with 20 ng/mL of TNF (Miltenyi Biotec Ltd).  
373 Healthy T and B cells were purified from PBMCs using CD3 (negative purification) or CD19 magnetic beads (Miltenyi Biotec Ltd), then activated  
374 with 1  $\mu$ g/mL phytohemagglutinin or 1  $\mu$ M of TLR9 ligand ODN 2006 (Miltenyi Biotec Ltd) respectively for 24h. Mouse anti-human CD69 antibody  
375 (clone FN50, BioLegend, San Diego, CA, USA) confirmed activation.

376

#### 377 *T cell clones*

378 HLA-A\*0201 restricted clone MEL5 recognizing peptides EAAGIGILTV and ELAGIGILTV (heteroclitic L at position 2) from Melan A<sup>29,30</sup> and a  
379 canonical MAIT clone were cultured as described previously<sup>31</sup>. Clone 40E.22 was confirmed as CD1a-restricted using CRISPR-Cas9 ablation of  
380 CD1a, b, c or d (data not shown).

381

#### 382 *Mycobacterium smegmatis and Salmonella Typhimurium*

383 Bacterium was grown and used to load phagocytic A549 as previously described<sup>37</sup>.

384

#### 385 *MC.7.G5 isolation and cloning*



386 PBMCs were isolated by standard density gradient centrifugation and labelled with proliferation dye carboxyfluorescein succinimidyl ester (CFSE)  
387 (eBiosciences™, Thermo Fisher Scientific, Leicestershire, UK) and cultured for two weeks with A549 cells in priming medium (R10 supplemented  
388 with 20 IU/mL IL-2 (Proleukin®; Prometheus, San Diego, CA), 1X MEM non-essential amino acids, 1 mM sodium pyruvate and 10 mM HEPES  
389 buffer (Thermo Fisher Scientific). Primed PBMC were bulk sorted for CFSE<sup>low</sup> viable CD3<sup>+</sup> CD4<sup>neg</sup> cells on a BD FACS Aria (BD Biosciences, Franklin  
390 Lakes, NJ, USA) and cloned by plating 0.3 cells/well in 96U-well plates.

391

#### 392 *T cell activation assays*

393 T cells were rested in R5 (as for R10 with 5% FBS) for 24 h prior to assay. Typically, 3 x10<sup>4</sup> T cells and 6 x10<sup>4</sup> target cells were used per well in R5  
394 and incubated overnight, with supernatants harvested for an Enzyme-Linked Immunosorbent Assay (ELISA) (MIP-1β or TNF), which were  
395 performed according to the manufacturer's instructions (R&D Systems, Biotechne, Minneapolis, MN, US). For antibody blocking assays, target  
396 cells were pre-incubated with anti-MR1 (clone 26.5, BioLegend), pan anti-MHCI (clone W6/32, BioLegend) or pan anti-MHCII (clone Tü39,  
397 BioLegend) antibodies before incubating with T cells. Staining for surface CD107a<sup>32</sup> using an anti-CD107a PE Ab (H4A3, BD Biosciences), and  
398 intracellularly with Abs for anti-TNF PE-Vio770 (clone cA2, Miltenyi Biotec Ltd) and anti-IFNγ (clone 45-15, Miltenyi Biotec Ltd), was performed as  
399 described previously<sup>31</sup>, following activation for 4 h at a T cell to target cell ratio of 1:1. Intracellular cytokine staining (ICS) was performed  
400 according to the manufacturer's instructions using a Cytofix/Cytoperm kit, GolgiPlug and GolgiStop (BD Biosciences). For tumor necrosis factor  
401 (TNF) processing inhibitor TAPI-0 (Santa Cruz Biotechnology, Dallas, Texas, USA) assays<sup>33</sup>, T-cells and target cells were co-incubated for 4 h with  
402 30 μM TAPI-0 and antibody directed against TNF (clone cA2, Miltenyi Biotec Ltd.). CD107a antibody (clone H4A3, Miltenyi Biotec Ltd.) was also

403 included at the start of the assay to detect activation induced degranulation of cytotoxic T-cells<sup>32</sup>. Following incubation, cells were washed and  
404 stained with Fixable Live/Dead Violet Dye and antibodies against T-cell surface markers. Gating strategy and isotype Ab (as recommended by the  
405 manufacturer of the primary Abs) control experiments for the TAPI-0 assay are shown in **Supplementary Fig. 7**. Ac-6-FP (Schircks Laboratories,  
406 Switzerland) was reconstituted in DMSO to 50 mg/mL and stored at -20°C protected from light. For MR1 loading Ac-6-FP was incubated  
407 overnight at 37°C and 5% CO<sub>2</sub> with target cells in their respective media.

408

#### 409 *Cytotoxicity assays*

410 For Cr<sup>51</sup> release cytotoxicity assays target cells were labelled with chromium-51 (Perkin Elmer, Waltham, Massachusetts, USA) then co-incubated  
411 with T cells at various T cell-to-target ratios for 6 or 18 h and specific lysis calculated, as described previously<sup>31</sup>. For flow-based killing assays  
412 5,000-10,000 cancer or healthy cell lines were plated in 96U well plates, and MC.7.G5 added to give the desired T cell to cell line ratio  
413 (experimental wells). The cells were co-cultured in 200 µL of target cell media supplemented with 20 IU of IL-2 and 25 ng/mL of IL-15. Targets  
414 cells (control wells), MC.7.G5 and CSFE CIRs were also cultured alone to aid analysis. The cells were incubated for 48 h or 7 d and fed (50% media  
415 change) twice for the latter. Prior to harvest, either BD negative CompBeads (BD Biosciences) (1 drop in 100 µL of PBS then 25 µL per well) or 0.1  
416 x10<sup>6</sup> CFSE labelled (0.1 µM) CIR cells were added to each well to allow the number of target cells that remained in experimental and control  
417 wells to be quantified. The cells were washed 3 times with chilled D-PBS EDTA (2 mM) then stained in the assay plates with Fixable Live/Dead Violet  
418 Dye (VIVID, Thermo Fisher Scientific) then CD3 PerCP (clone UCHT1, BioLegend) and/or anti-TRBV25.1 APC TCR (TRBV11 Arden nomenclature:

clone C21, Beckman Coulter, Brea, California, USA) Abs to allow dead cells and T cells to be gated-out leaving viable target cells for analyses  
(**Supplementary Fig. 7**). Percentage killing was calculated using the following equation:

$$\% \text{ killing} = 100 - \left( \left( \frac{\text{experimental target cell events} \div \text{experimental bead or CFSE C1R events}}{\text{control target cell events} \div \text{control bead or CFSE C1R events}} \right) \times 100 \right)$$

#### Flow Cytometry

Cells were stained with Fixable Live/Dead Violet Dye VIVID and the following surface antibodies: pan- $\alpha\beta$  TCR PE (clone IP26, BioLegend), pan- $\gamma\delta$  TCR-FITC (clone REA591, Miltenyi Biotec Ltd), CD3 PerCP (clone UCHT1), CD4 APC (clone VIT4, Miltenyi Biotec Ltd), CD8 PE (clone BW135/80, Miltenyi Biotec Ltd), rat CD2 PE (clone OX-34, BioLegend) and MR1 PE (clone 26.5, BioLegend). For staining with MR1 PE, FcR Block (Miltenyi Biotec Ltd) was used according to manufacturer's instructions and isotype Ab as described previously<sup>11</sup>. For tetramer staining, MR1 monomers were provided by Jamie Rossjohn (Monash University), and pMHC monomers produced in-house. Tetramers were assembled and used for optimized staining as described previously<sup>31</sup>. Cells were gated on lymphocytes (FSC-A versus SSC-A), single cells (FSC-A versus FSC-H) then viable cells (marker of choice versus VIVID) as show in **Supplementary Fig. 7**. Data was acquired on a BD FACS Canto II (BD Biosciences) and analysed with FlowJo software (Tree Star Inc., Ashland, OR, USA).

#### MR1 knockout and transgene expression

MR1 single guide (sg)RNA and CRISPR/Cas9 lentivirus was produced and used as described previously<sup>37</sup>. The native MR1 transgene was cloned into the second generation pRRL.sin.cppt.pgk-gfp.wpre lentivector backbone developed by Didier Trono's laboratory (Addgene #12252) devoid

434 of the human PGK promoter and GFP cDNA. The codon-optimised MR1 K43A transgene was cloned into the third generation pELNS vector  
435 (kindly provided by James Riley, University of Pennsylvania, PA) devoid of GFP cDNA. Lentiviral particles for native MR1 and MR1 K43A were  
436 produced by calcium chloride transfection of HEK293T cells, as described for MR1 sgRNA<sup>37</sup>. Target cells were spininfected in the presence of 8  
437 µg/mL polybrene; 500 x *g* for 2 hours at 37°C<sup>32</sup>. Anti-MR1 antibody PE (clone 26.5, BioLegend) positive cells were magnetically enriched using  
438 anti-PE magnetic beads according to manufacturer's instructions (Miltenyi Biotec Ltd).

439

#### 440 *TCR sequencing and transduction*

441 MC.7.G5 TCR was sequenced in-house using the SMARTer RACE kit (Takara Bio USA Holdings, Inc, Mountain View, CA, USA) and 2-step  
442 polymerase chain reaction using universal forward primers and reverse primers specific for TCR-α and TCR-β constant regions. The TCR was then  
443 synthesised with codon optimisation (Genewiz, South Plainfield, NJ, USA), with full length α and β TCR chains separated by a 'self-cleaving' T2A  
444 sequence<sup>33</sup> and cloned in to the third generation pELNS lentiviral vector containing rCD2 as a co-marker (kindly provided by James Riley,  
445 University of Pennsylvania, PA); the β TCR chain was separated from rCD2 by a P2A self-cleavage sequence (**Supplementary fig 6**). MC.7.G5 TCR-  
446 rCD2 pELNs was used to produce virus with envelope plasmid pMD2.G (Addgene plasmid #12259), and packaging plasmids pMDLg/pRRE  
447 (Addgene plasmid #12251) and pRSV-Rev (Addgene plasmid #12253) (all gifts from Didier Trono). Lentiviral particles were generated by calcium  
448 chloride transfection of HEK293T cells and the supernatant 0.4 µm filtered then concentrated by ultra-centrifugation (150,000 g 2h 4°C). The  
449 concentrated lentiviral supernatants were resuspended in T-cell transduction media (as for priming media but with 20% FBS and 25 ng/mL of IL-  
450 15 (Miltenyi Biotec Ltd.)), used immediately, or stored at -80°C and only defrosted once before transduction. Post therapy PBMCs were obtained

451 from TIL patients MM909.11 and MM909.24 and CD8 and CD4 T cells purified by magnetic enrichment (Miltenyi Biotec Ltd). T cells ( $1-1.5 \times 10^6$ )  
452 were then activated by overnight incubation with CD3/CD28 beads (Dynabeads; Thermo Fisher Scientific) at a 3:1 bead-to-T cell ratio in 2 mL of  
453 T-cell transduction media in 24 well plates. The following day, 900  $\mu$ L of the media was removed and replaced with 500  $\mu$ L of MC.7.G5 TCR  
454 lentivirus supernatant in the presence of 5  $\mu$ g/mL polybrene (Santa Cruz Biotechnology, Dallas TX, USA). Seven days later, T cells that had taken  
455 up the virus were magnetically enriched with anti-rCD2 PE conjugated antibody and anti-PE magnetic beads, according to manufacturer's  
456 instructions (Miltenyi Biotec Ltd). Fourteen days post-transduction, T cells were expanded as described previously<sup>31</sup> and used for assays after 2  
457 weeks.

458

#### 459 *Whole genome GeCKOv.2 screening*

460 Lentiviral particles for the GeCKOv.2 library (plasmid kindly provided by Feng Zhang<sup>34</sup> (Addgene plasmid #1000000048)). The GeCKOv.2 library  
461 consists of 123,411 sgRNAs targeting 19,050 protein-coding genes (6 sgRNAs per gene) and 1,864 microRNAs (4 sgRNAs per microRNA) and was  
462 used as lentivirus to transduce the target cell line HEK293T.  $4 \times 10^7$  HEK-293T cells were transduced with a MOI of 0.4 to provide 100X coverage  
463 of each sub-library. Cells that had taken up the lentivirus were selected under puromycin. After 14 days, half the library-containing cells were  
464 frozen as a control. MC.7.G5 was added to remaining transduced HEK-293T cells at a T cell to HEK293T ratio of 0.25:1 in 20 IU IL-2 media. After  
465 14 days, MC.7.G5 was added again at a 0.5:1 ratio. After 7 days the HEK293T cells were used for sequencing. Genomic DNA from  $3 \times 10^7$  of HEK-  
466 293T cells (unselected control and selected with MC.7.G5) was isolated (GenElute Mammalian Genomic DNA Miniprep Kit, Sigma-Aldrich, Merck  
467 KGaA, St Louis, Missouri, USA). The entirety of isolated genomic DNA (2.5  $\mu$ g per 50  $\mu$ l reaction) was used for subsequent PCR, to ensure

468 capturing the full representation of the libraries. The two step PCR was performed as described before (19), using HPLC purified primers and  
469 NEBNext High Fidelity PCR MasterMix (New England Biolabs, Ipswich, MS, USA). The <300 bp PCR products were subsequently isolated from the  
470 agarose gel and sequenced on HiSeq instrument (Illumina, San Diego, CA, USA), with 80 cycles of read 1 (to determine the sequence of sgRNAs)  
471 and 8 cycles of read 2 (to identify sample-specific barcode). Analysis of enriched guides was performed using MAGeCK analysis<sup>35</sup>.

#### 472 *Cell stress assays*

473 Cells were harvested from culture then incubated with 100-200  $\mu$ M tert-Butyl hydroperoxide (tBHP) or hydrogen peroxide (H<sub>2</sub>O<sub>2</sub>) for 1h in R10,  
474 followed by staining with CellROX green reagent to detect reactive oxygen species (ROS), according to the manufacturer's instructions (Thermo  
475 Fisher Scientific). Cells were also stained with viability stain VIVID as above. Caesium source  $\gamma$ -irradiation of cells was performed using a Gamma  
476 Cell irradiator. *M. smeg* infection of healthy lung epithelial cells was performed as for A549s described above.

477

#### 478 *Mouse Experiments*

479 Female JAX<sup>TM</sup> NOD *scid* gamma (NSG<sup>®</sup>) were purchased from Charles Rivers (Wilmington, MA, US) at 6-7 weeks of age, housed under specific  
480 pathogen free conditions and experiments initiated within one week of arrival. Experiments were performed under United Kingdom Home  
481 Office approved projects 30/3188 and P2FB675AB conducted in compliance with the United Kingdom Home Office Guidance on the Operation of  
482 the Animals (Scientific Procedures) Act 1986. Jurkat cells expressing DsRed-Express2 were generated using pELNS vector and lentiviral particles  
483 as described above then cloned. Prior to *in vivo* transfer Jurkat-DsRed cells and MC.7.G5 were depleted of dead or dying cells by standard

484 density gradient centrifugation. Jurkats cells ( $3 \times 10^6$ ) were engrafted first, followed by  $1.5 \times 10^6$  MC.7.G5 7d later. Cells were injected into the tail  
485 vein of mice using a 29G BD microfine syringe in 100  $\mu$ L of PBS. Mice that did not receive cells were injected with PBS. Each mouse (+/- T cells)  
486 received  $5 \times 10^4$  IU of IL-2 and 50  $\mu$ g of IL-15 (details as above) via injection into the peritoneal cavity on the day of T cell transfer and every 48h  
487 for the duration of the experiment. Bone marrow was harvested from the tibia and fibula, and splenocytes prepared for staining using standard  
488 density gradient centrifugation. Cells were stained with the viable dye VIVID, followed by antibodies for human CD3 and CD8 (details as above),  
489 and anti-human CD45 APC-Cy7 (clone HI30, BioLegend) and anti-mouse/human CD11b PE-Cy7 (clone M1/70, BD Biosciences) antibodies as  
490 described previously<sup>38</sup>. Gating strategy for analyses of flow cytometry data is shown in **Supplementary Fig. 8**. For Jurkat co-transfer experiments,  
491 *MR1*<sup>-/-</sup> DsRed-Express2<sup>+</sup> Jurkat cells were firstly generated as described above using the MR1 CRISPR-cas9, followed by cloning.  $2 \times 10^6$  WT and  
492 *MR1*<sup>-/-</sup> (DsRed-Express2<sup>+</sup>) Jurkats were transferred to the same mouse, then MC.7.G5 T cells ( $3 \times 10^6$ ) 7d later to the +T cell group. Splenocytes  
493 were harvested at 25d post T cell transfer then incubated with mouse and human FcR block (Miltenyi Biotec Ltd), stained with VIVID and  
494 antibodies for CD3, CD8, CD45, as above, and also with mouse anti-human pan HLA class I (clone W6/32, BioLegend). Survival of mice with Jurkat  
495 cells was assessed by monitoring body weight; mice were culled when they had lost  $\geq 15\%$  of their initial body weight according to United  
496 Kingdom Home Office stipulation.

497

#### 498 *Statistical analyses*

499 Neither blinding or randomization was performed for the *in vivo* studies. A two-sided non-parametric two-sample Kolmogorov-Smirnov test was  
500 used for Jurkat cell burden in NSG mice. The logrank two-sided p value and hazard ratio were calculated using the MatSurv survival analysis

501 function in Matlab, available at <https://www.github.com/aebergl/MatSurv>. The number of mice used in each group is indicated in the respective  
502 figure legend.

503  
504 **DATA AVAILABILITY**

505 The datasets generated during the current study are available from the corresponding author on reasonable request

506  
507 **Methods References**

- 508
- 509 1. Vavassori, S. *et al.* Butyrophilin 3A1 binds phosphorylated antigens and stimulates human  $\gamma\delta$  T cells. *Nat. Immunol.* **14**, 908–916 (2013).
  - 510 2. Kjer-Nielsen, L. *et al.* MR1 presents microbial vitamin B metabolites to MAIT cells. *Nature* **491**, 717–723 (2012).
  - 511 3. Corbett, A. J. *et al.* T-cell activation by transitory neo-antigens derived from distinct microbial pathways. *Nature* **509**, 361–5 (2014).
  - 512 4. Gold, M. C. *et al.* MR1-restricted MAIT cells display ligand discrimination and pathogen selectivity through distinct T cell receptor usage. *J.*  
513 *Exp. Med.* **211**, 1601–1610 (2014).
  - 514 5. Eckle, S. B. G. *et al.* Recognition of Vitamin B precursors and byproducts by mucosal associated invariant T cells. *J. Biol. Chem.* **290**, 30204–  
515 30211 (2015).
  - 516 6. Le Bourhis, L. *et al.* Antimicrobial activity of mucosal-associated invariant T cells. *Nat. Immunol.* **11**, 701–708 (2010).
  - 517 7. Reantragoon, R. *et al.* Structural insight into MR1-mediated recognition of the mucosal associated invariant T cell receptor. *J. Exp. Med.*  
518 **209**, 761–774 (2012).
  - 519 8. Lepore, M. *et al.* Parallel T-cell cloning and deep sequencing of human MAIT cells reveal stable oligoclonal TCR $\beta$  2 repertoire. *Nat.*  
520 *Commun.* **5**, 3866 (2014).
  - 521 9. Lepore, M. *et al.* Functionally diverse human T cells recognize non-microbial antigens presented by MR1. *Elife* **6**, 1–22 (2017).
  - 522 10. Gherardin, N. A. *et al.* Diversity of T Cells Restricted by the MHC Class I-Related Molecule MR1 Facilitates Differential Antigen Recognition.  
523 *Immunity* **44**, 32–45 (2016).
  - 524 11. Laugel, B. *et al.* Engineering of Isogenic Cells Deficient for MR1 with a CRISPR/Cas9 Lentiviral System: Tools To Study Microbial Antigen



- 525 Processing and Presentation to Human MR1-Restricted T Cells. *J. Immunol.* **197**, 971–982 (2016).
- 526 12. Keller, A. N. *et al.* Drugs and drug-like molecules can modulate the function of mucosal-associated invariant T cells. *Nat. Immunol.* (2017).  
527 doi:10.1038/ni.3679
- 528 13. Reantragoon, R. *et al.* Antigen-loaded MR1 tetramers define T cell receptor heterogeneity in mucosal-associated invariant T cells. *J. Exp.*  
529 *Med.* **210**, 2305–20 (2013).
- 530 14. McWilliam, H. E. G. *et al.* The intracellular pathway for the presentation of vitamin B–related antigens by the antigen-presenting molecule  
531 MR1. *Nat. Immunol.* **advance on**, 1–9 (2016).
- 532 15. Lamichhane R and Ussher JE. Expression and trafficking of MHC related protein 1 (MR1). *J. Immunol.* **38**, 42–49 (2017).
- 533 16. Young, M. H. *et al.* MAIT Cell Recognition of MR1 on Bacterially Infected and Uninfected Cells. *PLoS One* **8**, e53789 (2013).
- 534 17. Gentles, A. J. *et al.* The prognostic landscape of genes and infiltrating immune cells across human cancers. *Nat. Med.* **21**, 938–945 (2015).
- 535 18. Gherardin, N. A. *et al.* Enumeration, functional responses and cytotoxic capacity of MAIT cells in newly diagnosed and relapsed multiple  
536 myeloma. *Sci. Rep.* **8**, 4159 (2018).
- 537 19. Parra-Cuadrado, J. F. *et al.* A study on the polymorphism of human MHC class I-related MR1 gene and identification of an MR1-like  
538 pseudogene. *Tissue Antigens* **56**, 170–2 (2000).
- 539 20. Seshadri, C. *et al.* A polymorphism in human MR1 is associated with mRNA expression and susceptibility to tuberculosis. *Nat. Publ. Gr.* **18**,  
540 8–14 (2016).
- 541 21. Lion, J. *et al.* MR1B , a natural spliced isoform of the MHC-related 1 protein , is expressed as homodimers at the cell surface and activates  
542 MAIT cells. 1363–1373 (2013). doi:10.1002/eji.201242461
- 543 22. Shalem, O. *et al.* Genome-scale CRISPR-Cas9 knockout screening in human cells - supplement. *Science (80-. )*. **343**, 84–87 (2014).
- 544 23. Patel, S. J. *et al.* Identification of essential genes for cancer immunotherapy. *Nature* **548**, 537–542 (2017).
- 545 24. Reith, W., LeibundGut-Landmann, S. & Waldburger, J.-M. Regulation of MHC class II gene expression by the class II transactivator. *Nat.*  
546 *Rev. Immunol.* **5**, 793–806 (2005).
- 547 25. Eckle, S. B. G. *et al.* A molecular basis underpinning the T cell receptor heterogeneity of mucosal-associated invariant T cells. *J. Exp. Med.*  
548 **211**, 1585–1600 (2014).
- 549 26. Alía, M., Ramos, S., Mateos, R., Bravo, L. & Goya, L. Response of the antioxidant defense system to tert-butyl hydroperoxide and  
550 hydrogen peroxide in a human hepatoma cell line (HepG2). *J. Biochem. Mol. Toxicol.* **19**, 119–128 (2005).
- 551 27. Irvine, D. J., Purbhoo, M. A., Krogsgaard, M. & Davis, M. M. Direct observation of ligand recognition by T cells. *Nature* **419**, 845–849

552 (2002).

553 28. Hulin-Curtis, S. L. *et al.* Histone deacetylase inhibitor trichostatin A sensitises cisplatin-resistant ovarian cancer cells to oncolytic  
554 adenovirus. *Oncotarget* **9**, 26328–26341 (2018).

555 29. Wooldridge, L. *et al.* MHC Class I Molecules with Superenhanced CD8 Binding Properties Bypass the Requirement for Cognate TCR  
556 Recognition and Nonspecifically Activate CTLs. *J. Immunol.* **184**, 3357–3366 (2010).

557 30. Lissina, A. *et al.* Protein kinase inhibitors substantially improve the physical detection of T-cells with peptide-MHC tetramers. *J. Immunol.*  
558 *Methods* **340**, 11–24 (2009).

559 31. Tungatt, K. *et al.* Antibody Stabilization of Peptide-MHC Multimers Reveals Functional T Cells Bearing Extremely Low-Affinity TCRs. *J.*  
560 *Immunol.* **194**, 463–474 (2014).

561 32. Betts, M. R. *et al.* Sensitive and viable identification of antigen-specific CD8+ T cells by a flow cytometric assay for degranulation. *J.*  
562 *Immunol. Methods* **281**, 65–78 (2003).

563 33. Haney, D. *et al.* Isolation of viable antigen-specific CD8+ T cells based on membrane-bound tumor necrosis factor (TNF)- $\alpha$  expression. *J.*  
564 *Immunol. Methods* **369**, 33–41 (2011).

565 34. Shalem, O. *et al.* Genome-scale CRISPR-Cas9 knockout screening in human cells. *Science (80-. ).* **343**, 84–87 (2014).

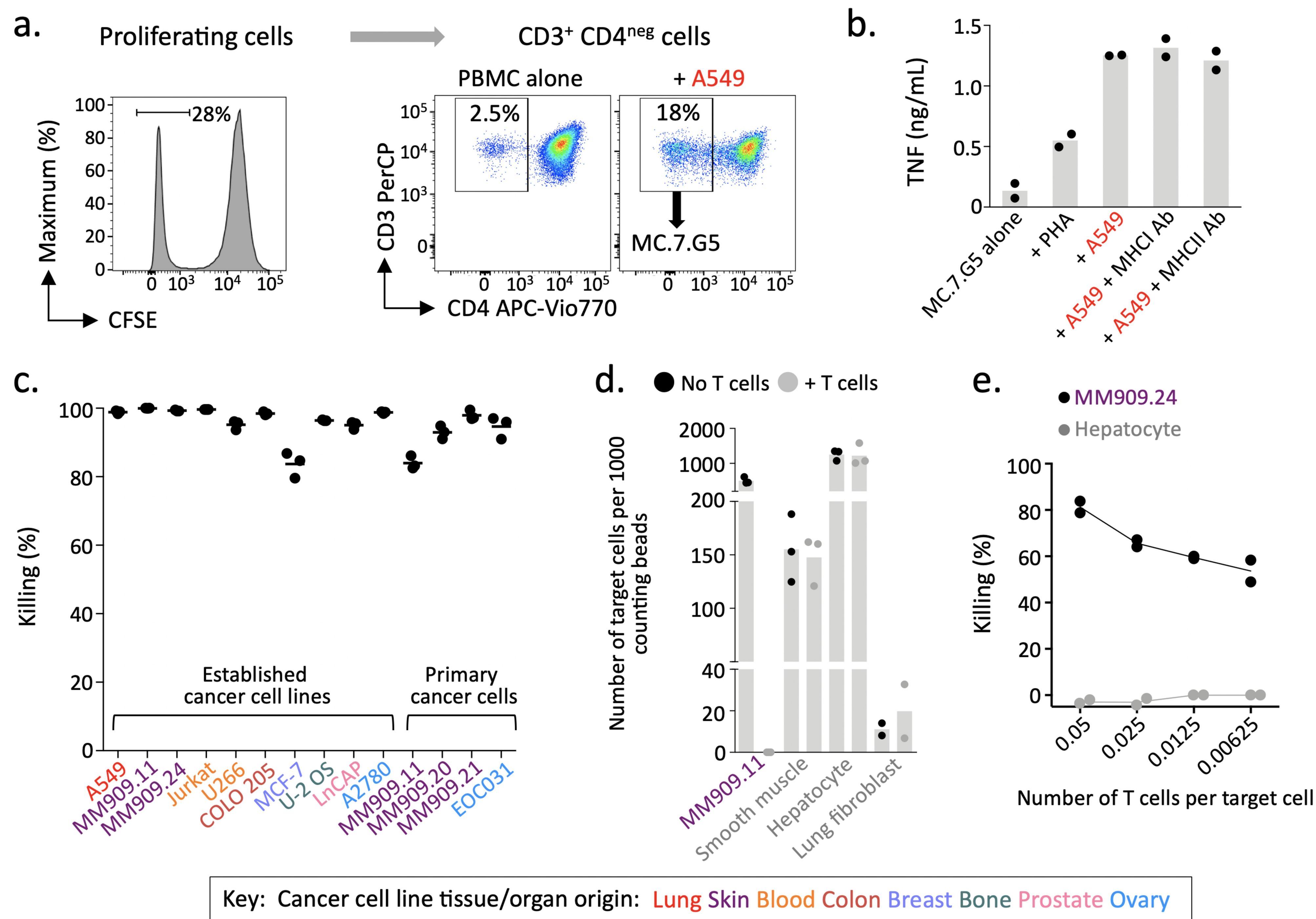
566 35. Ryan, M. D., King, A. M. Q. & Thomas, G. P. Cleavage of foot-and-mouth disease virus polyprotein is mediated by residues located within a  
567 19 amino acid sequence. *J. Gen. Virol.* **72**, 2727–2732 (1991).

568 36. Sanjana, N. E., Shalem, O. & Zhang, F. Improved vectors and genome-wide libraries for CRISPR screening. *Nat. Methods* **11**, 783–784  
569 (2014).

570 37. Li, W. *et al.* MAGeCK enables robust identification of essential genes from genome-scale CRISPR/Cas9 knockout screens. *Genome Biol.* **15**,  
571 554 (2014).

572 38. Maciocia, P. M. *et al.* Targeting the T cell receptor  $\beta$ -chain constant region for immunotherapy of T cell malignancies. *Nat. Med.* (2017).  
573 doi:10.1038/nm.4444

574



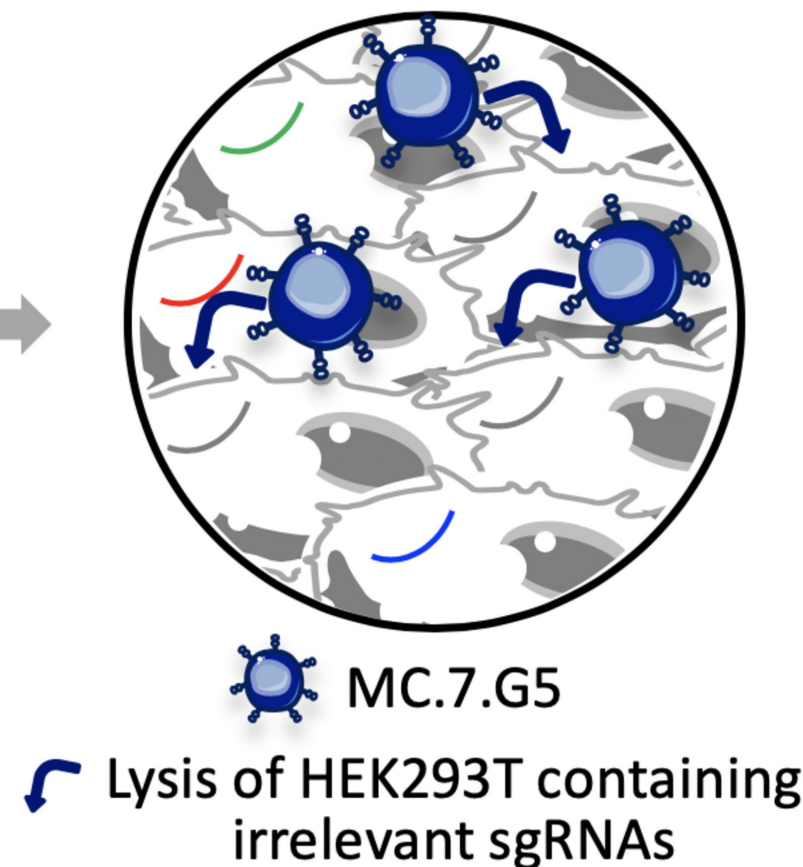
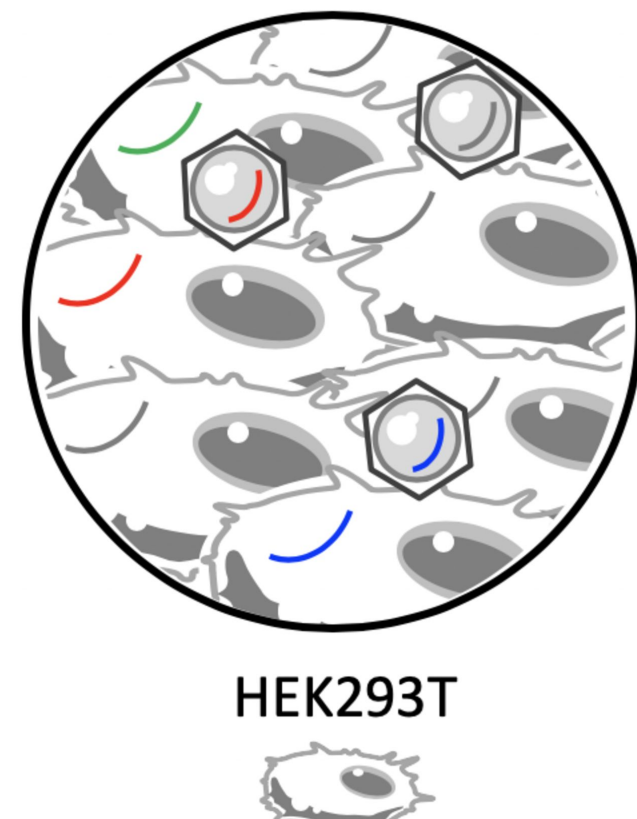
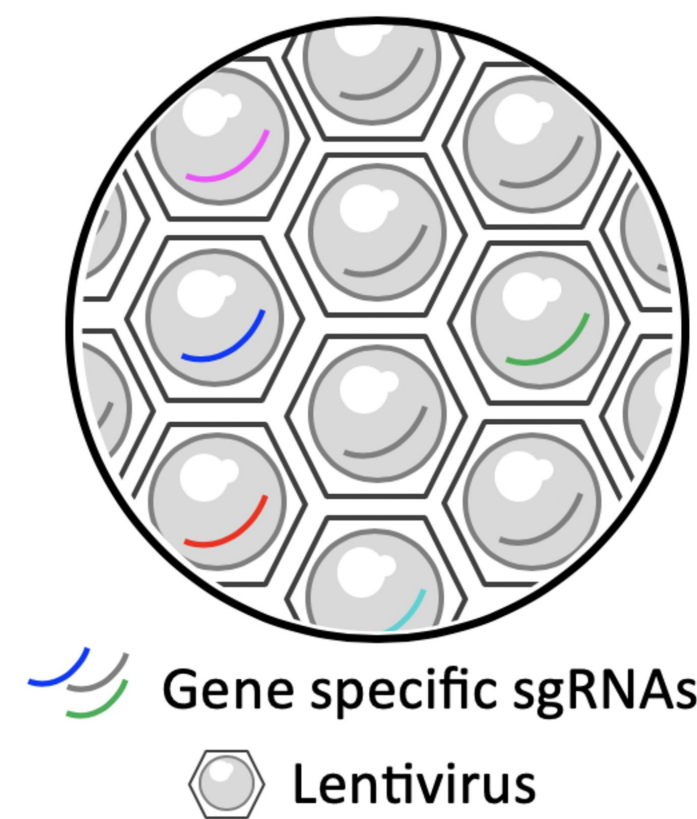


a.

Whole genome CRISPR-Cas9  
lentivirus libraries (A & B)

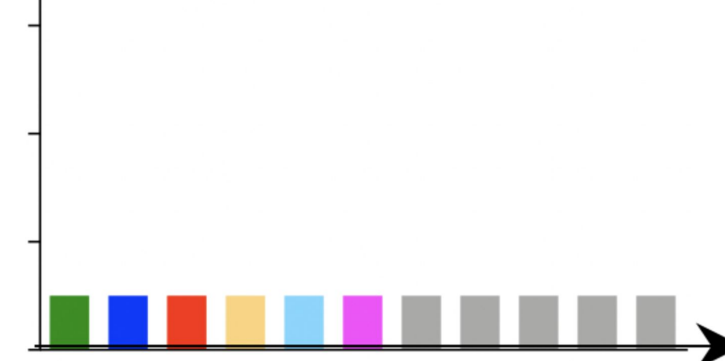
Transduced target cell  
libraries (A & B)

Selection with  
T-cell clone

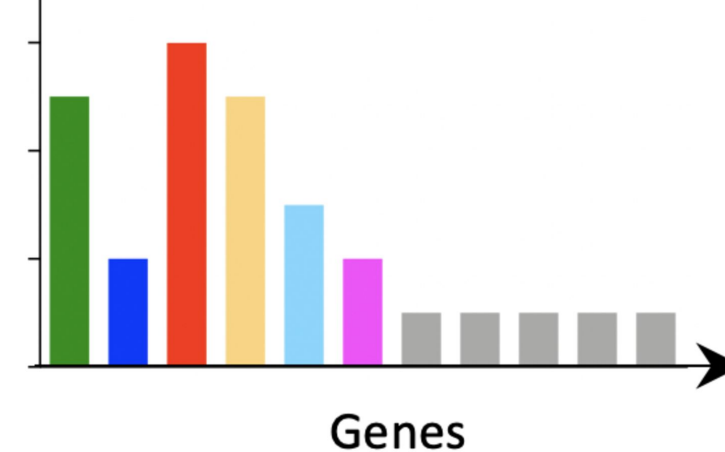


Number of different gRNAs per gene

Unselected libraries  
No MC.7.G5



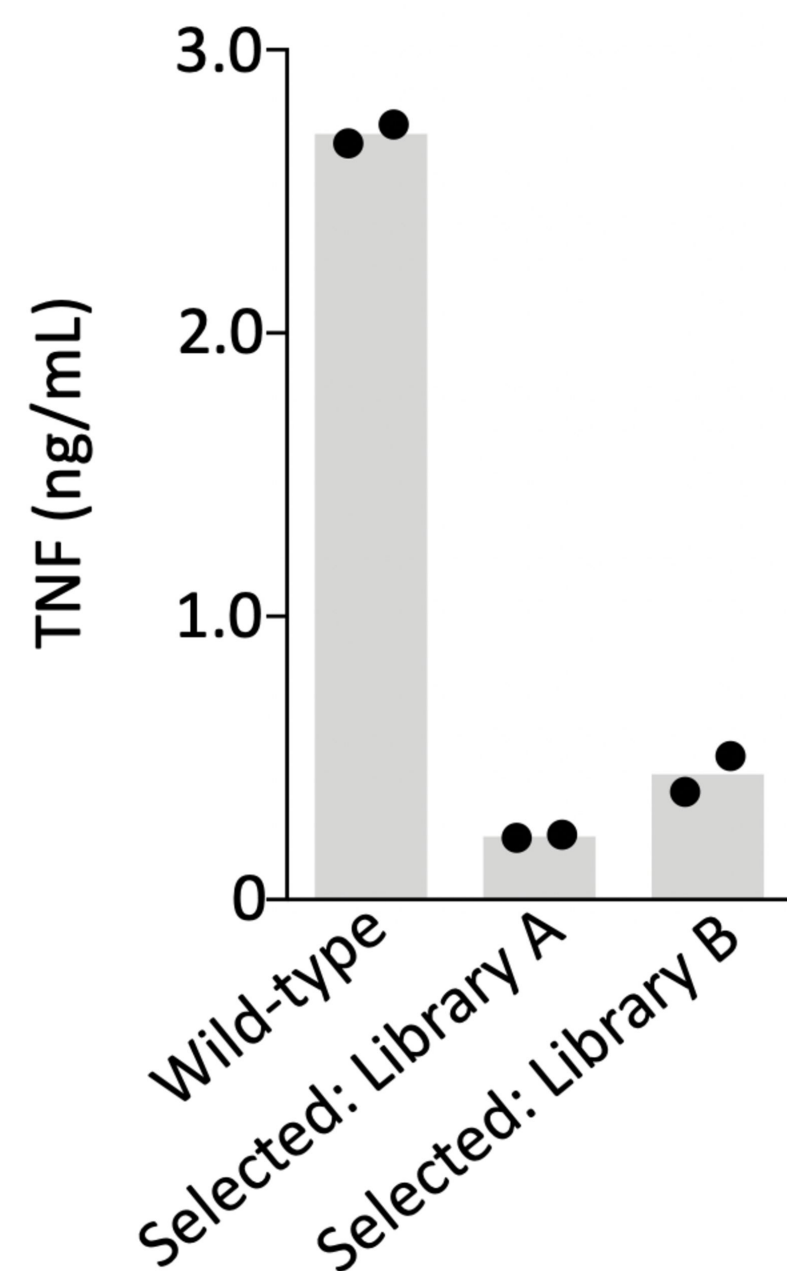
Selected libraries  
+ MC.7.G5



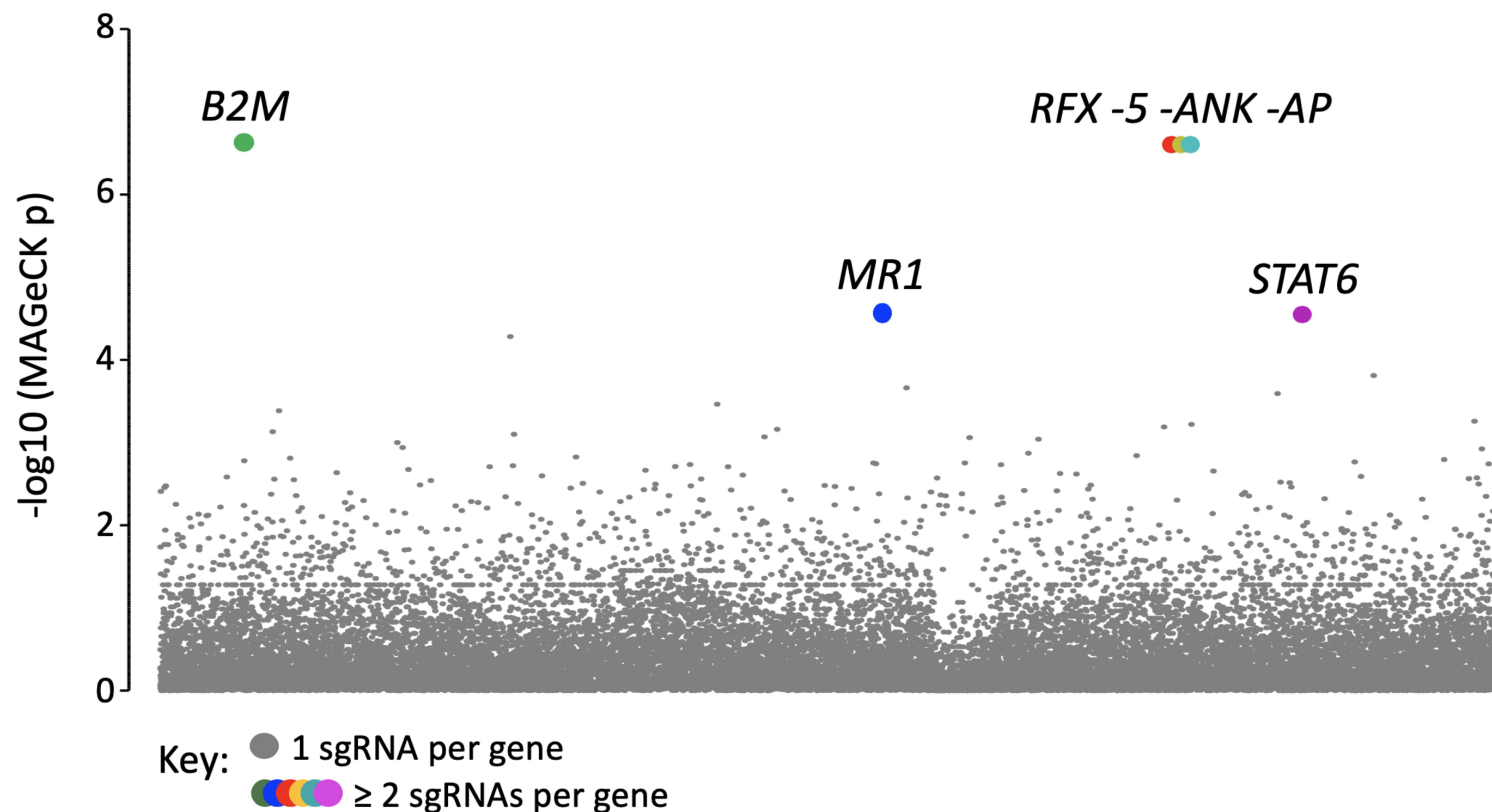
Comparison

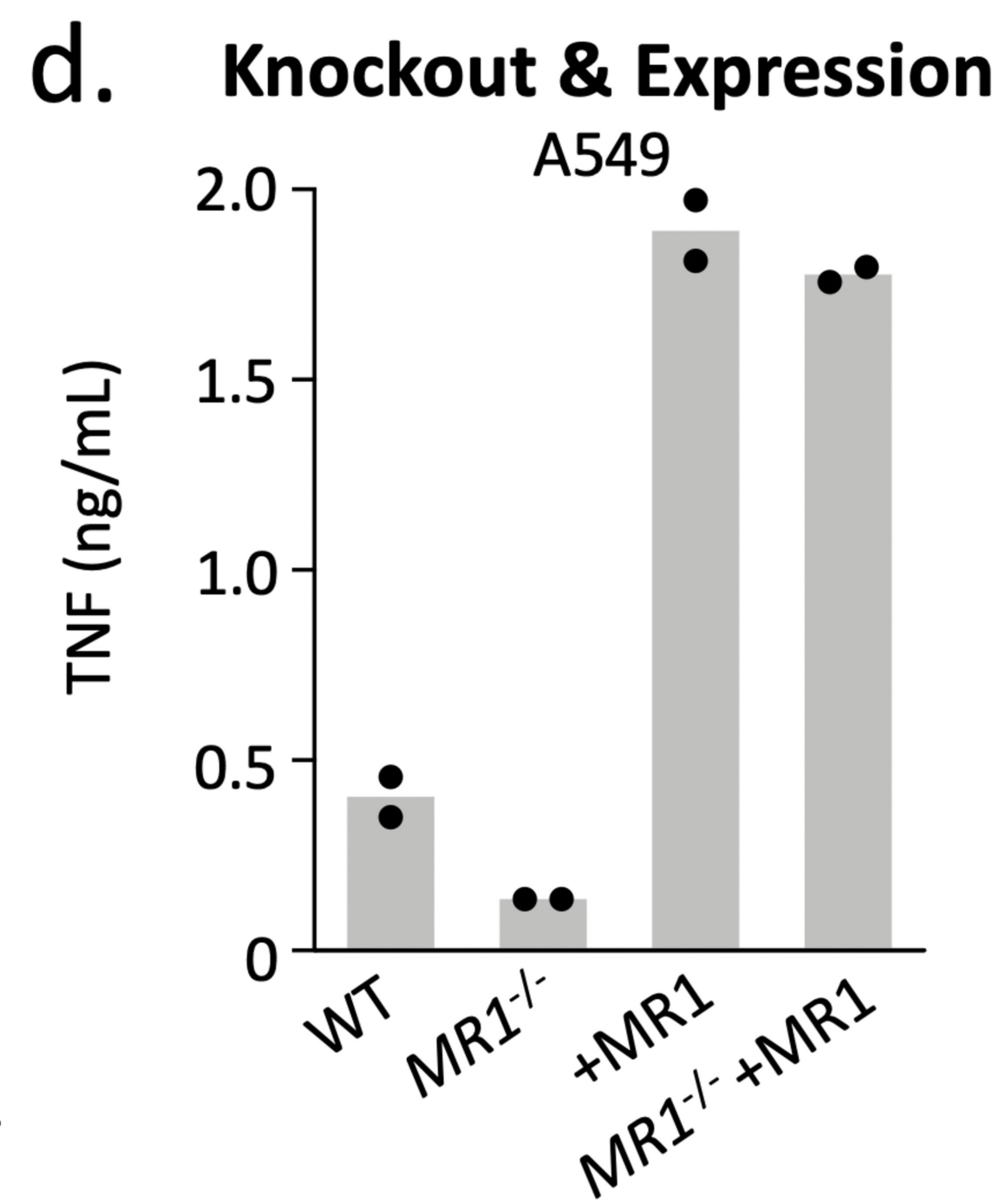
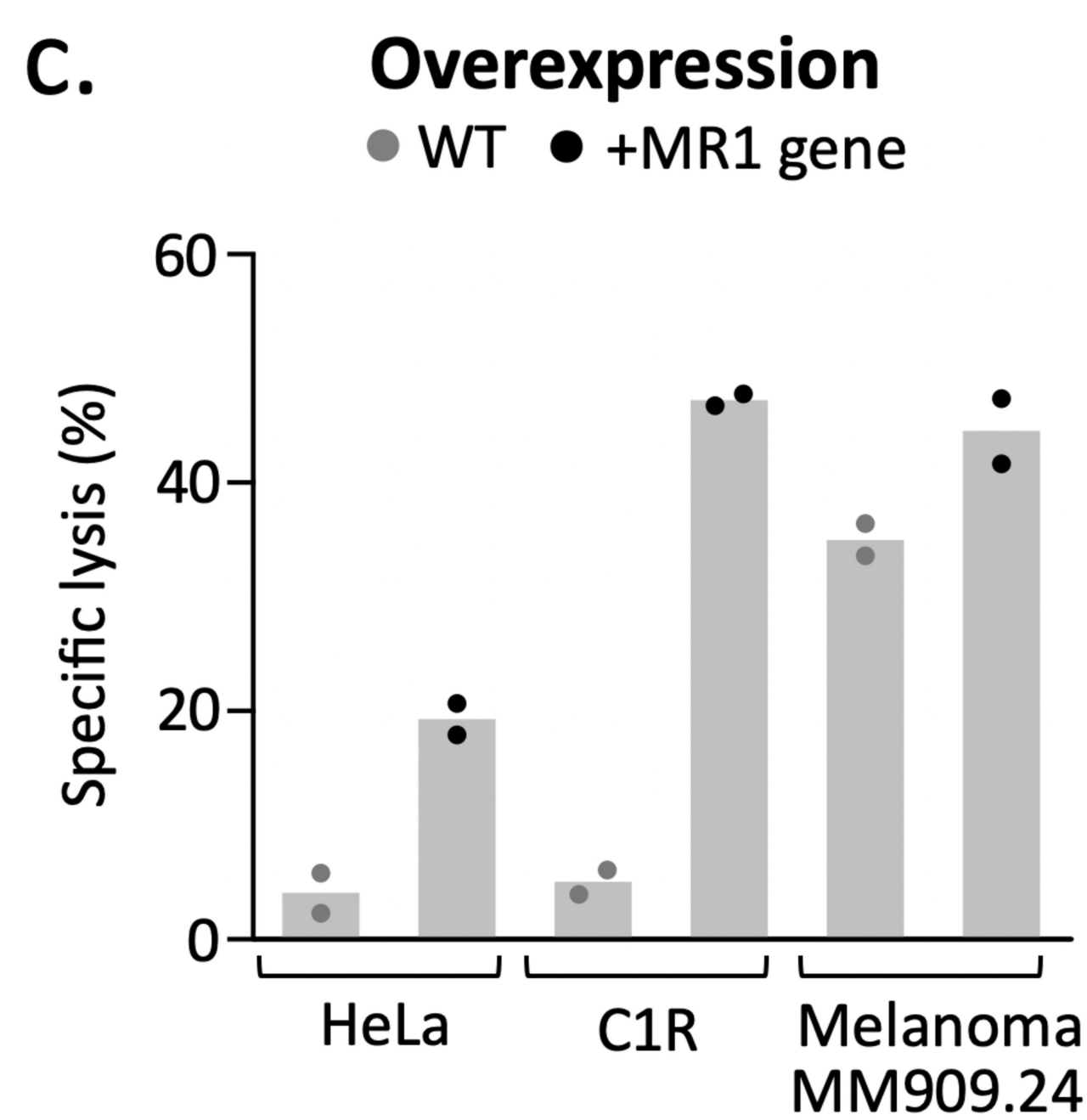
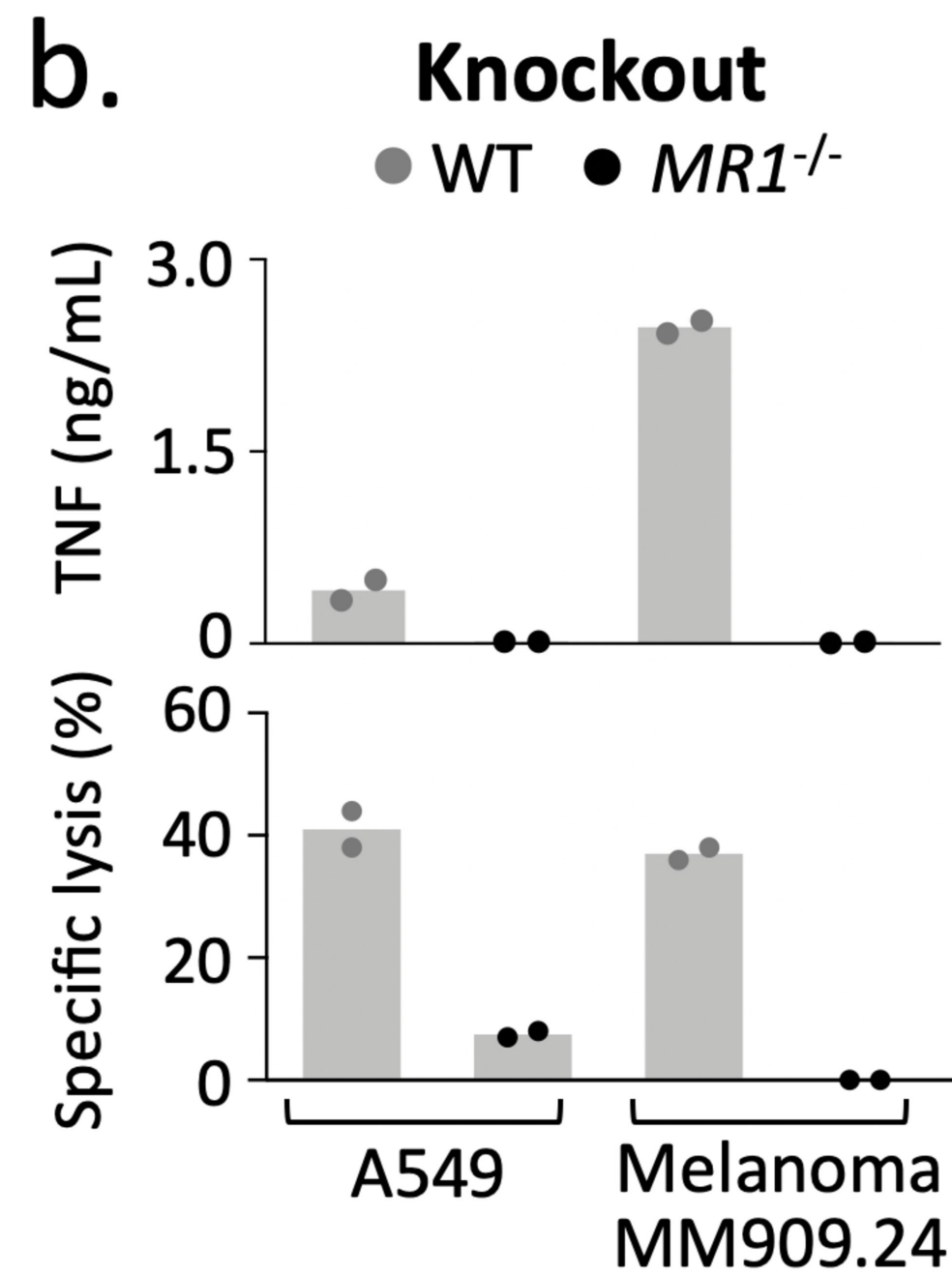
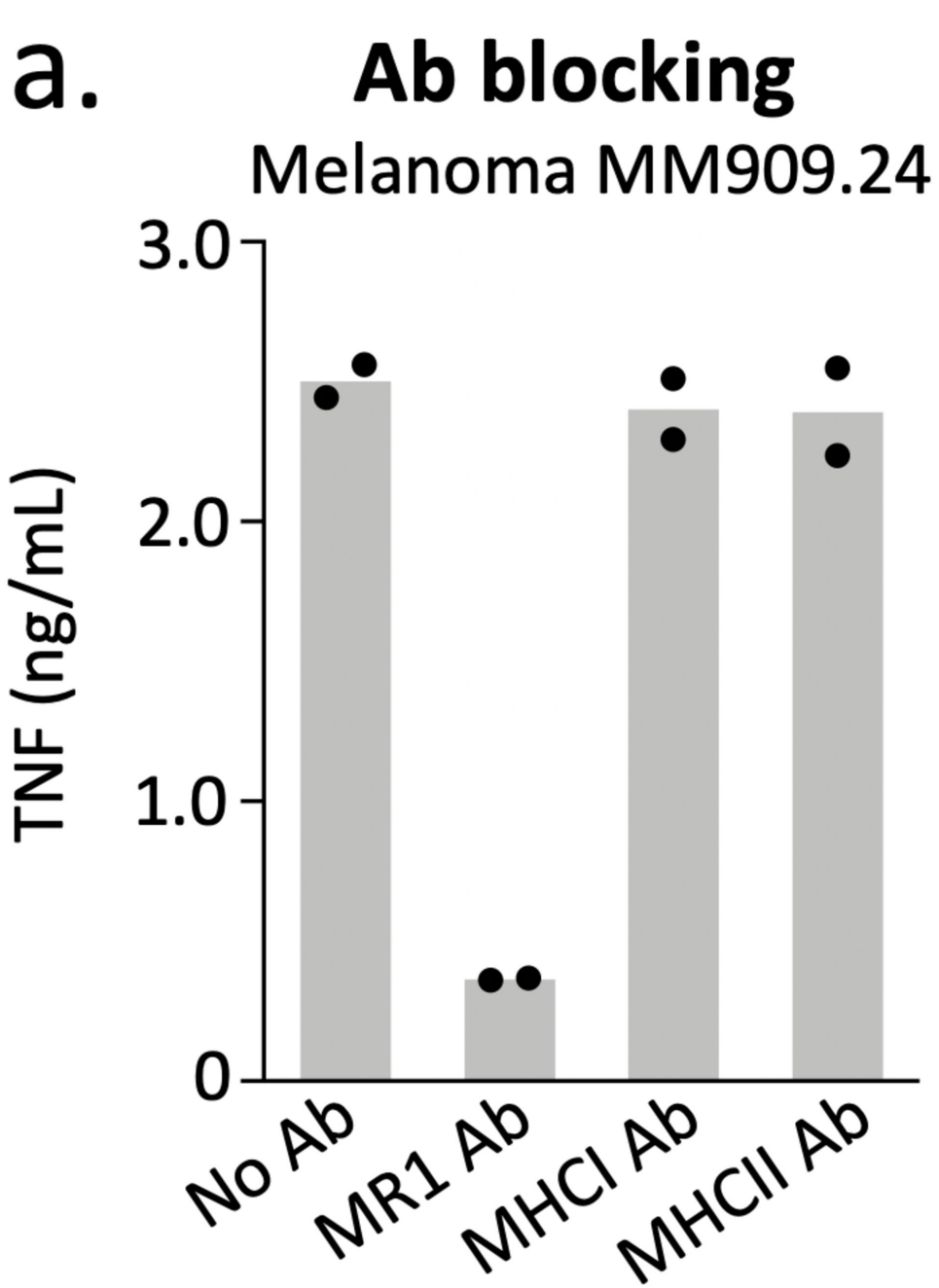
b.

MC.7.G5 versus HEK293T

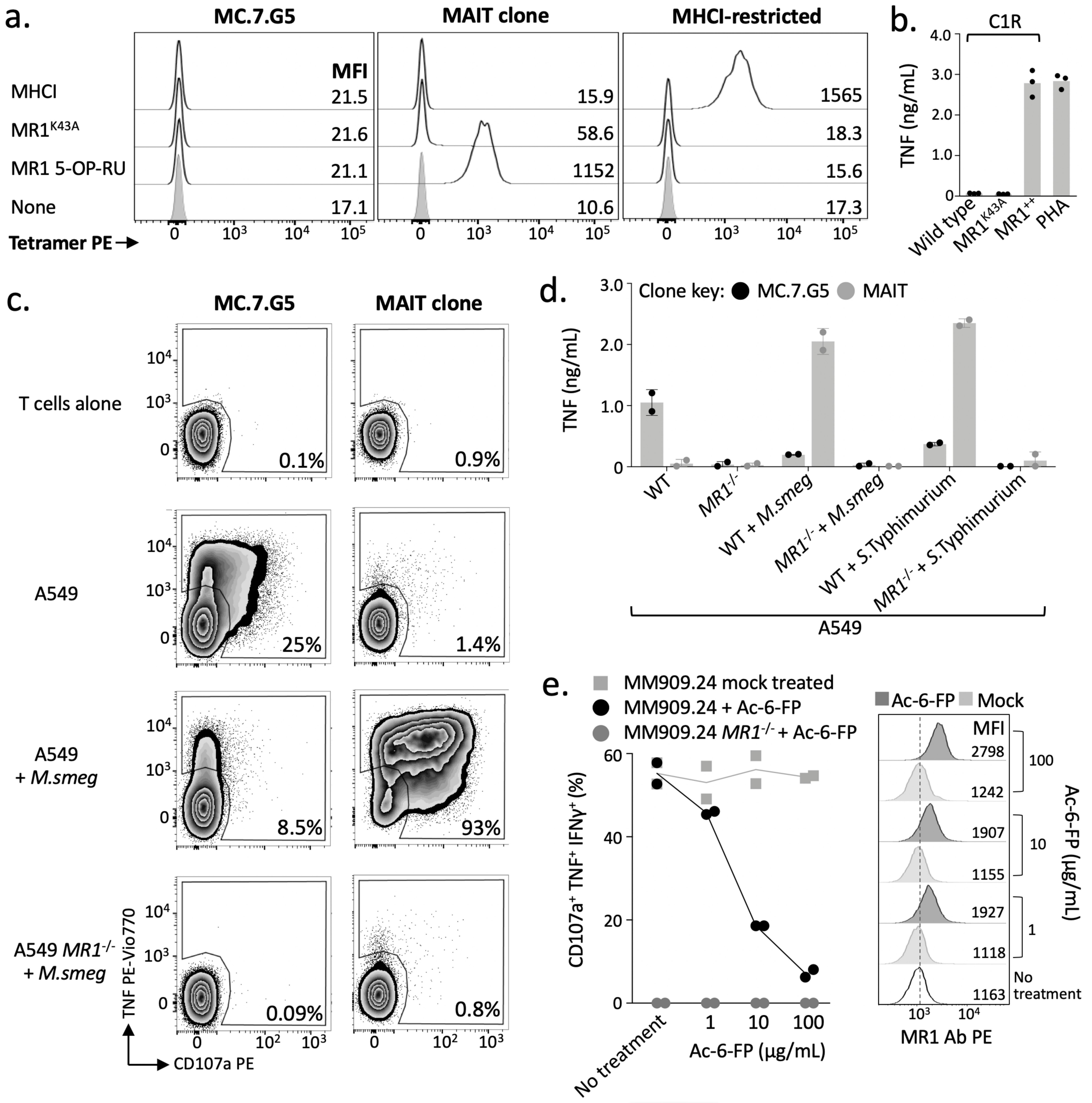


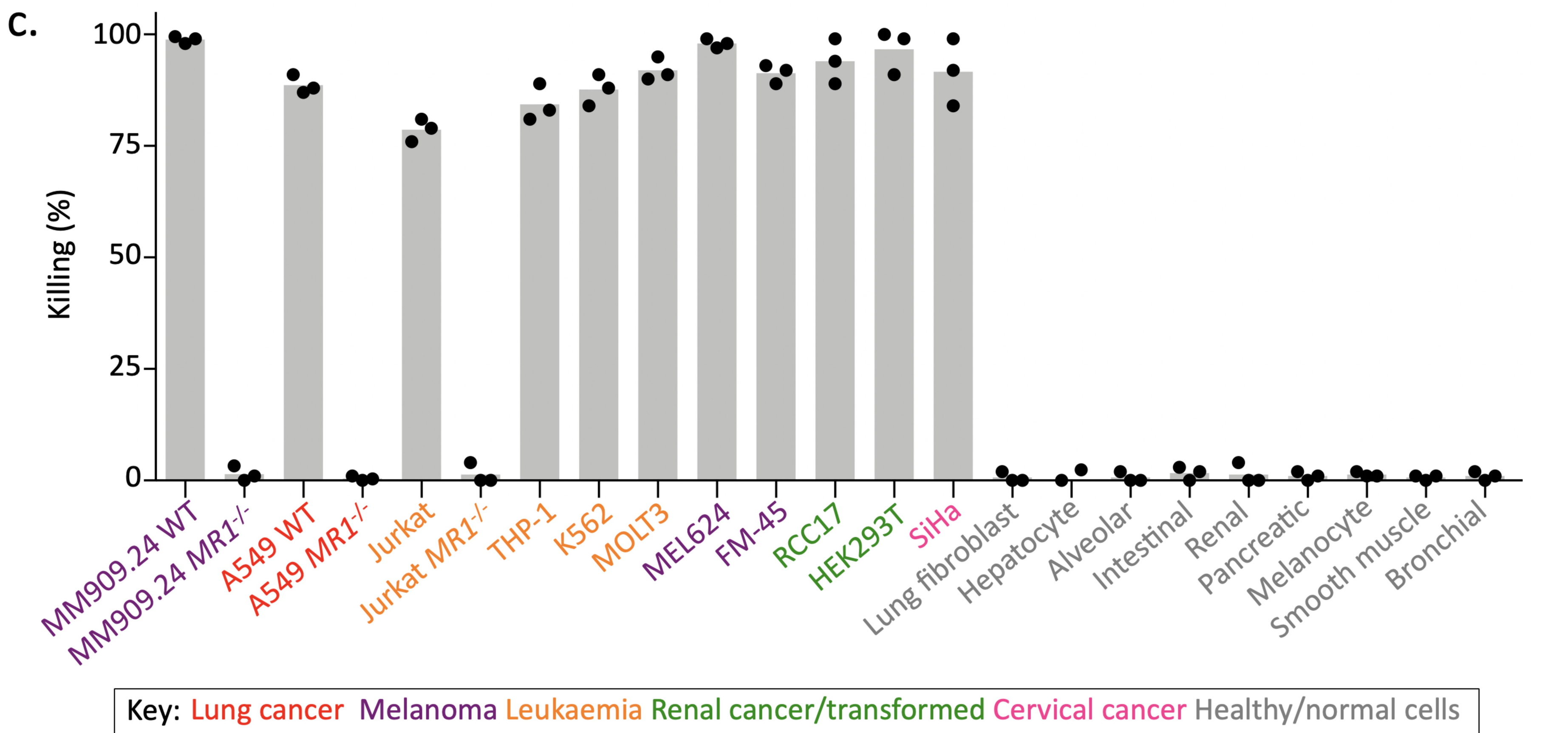
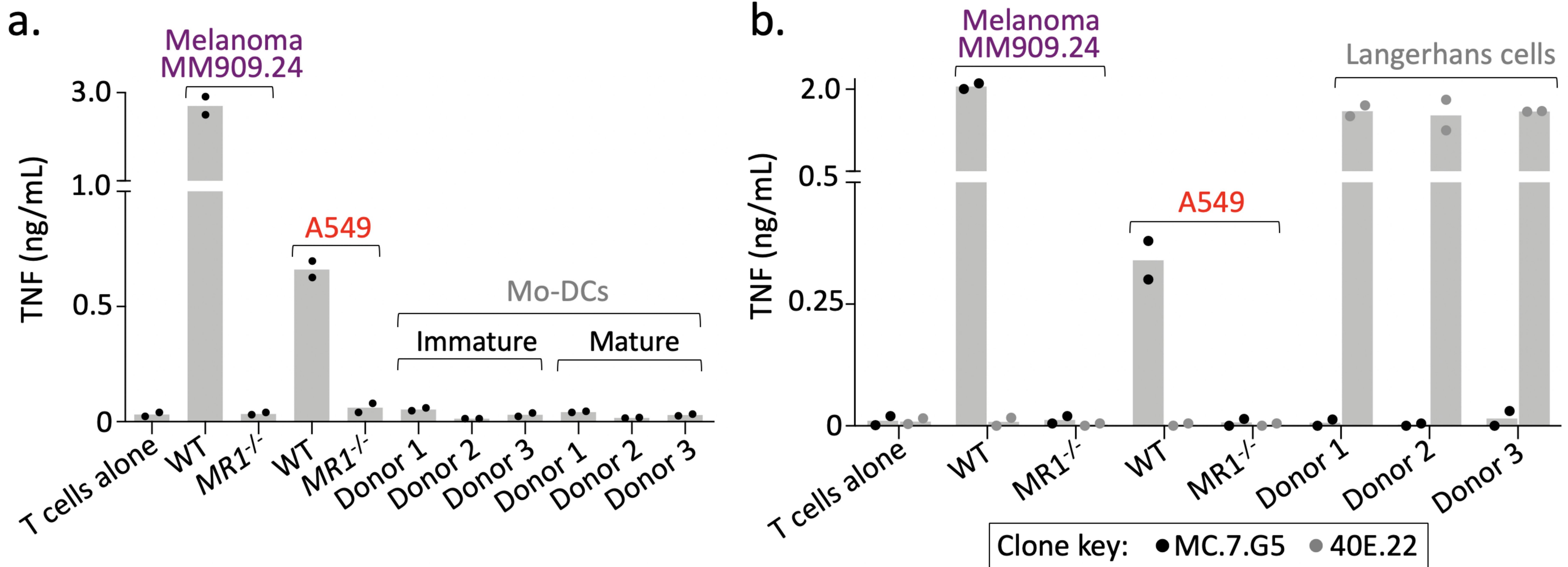
c.



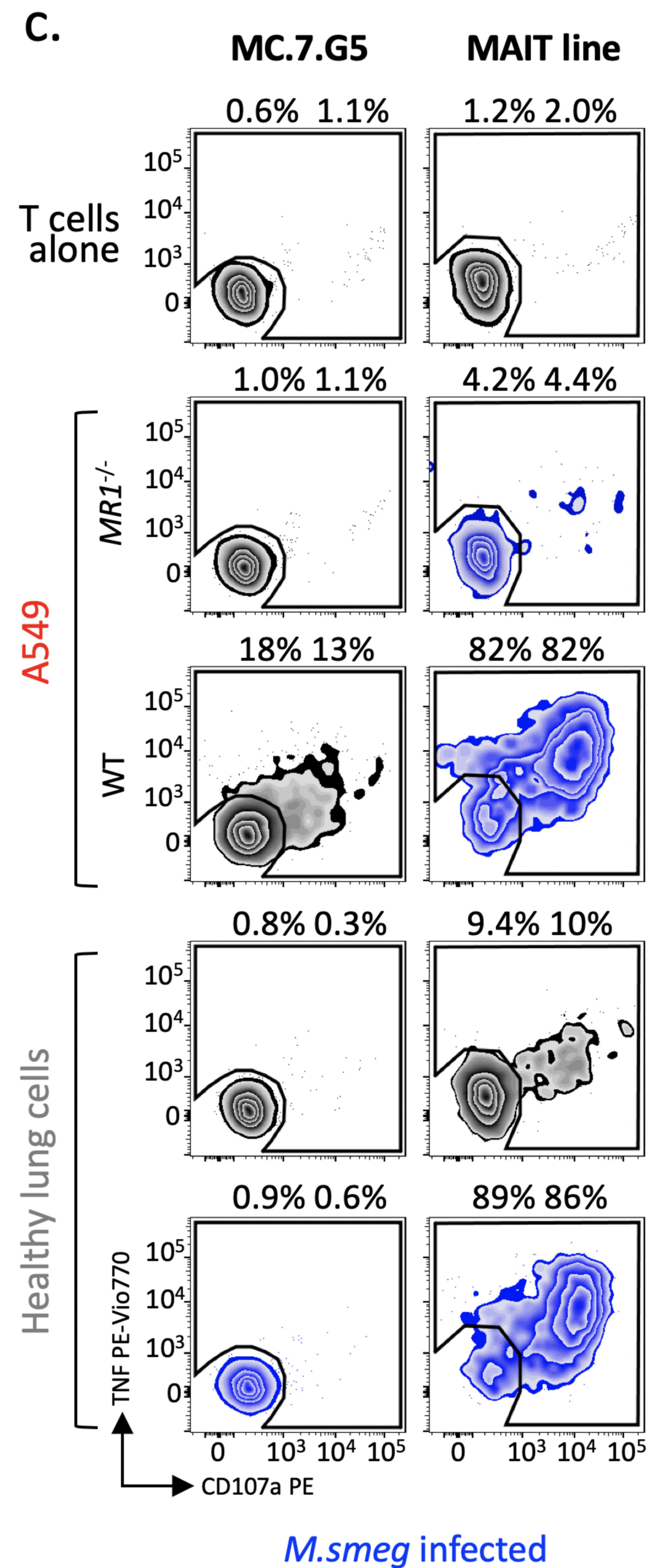
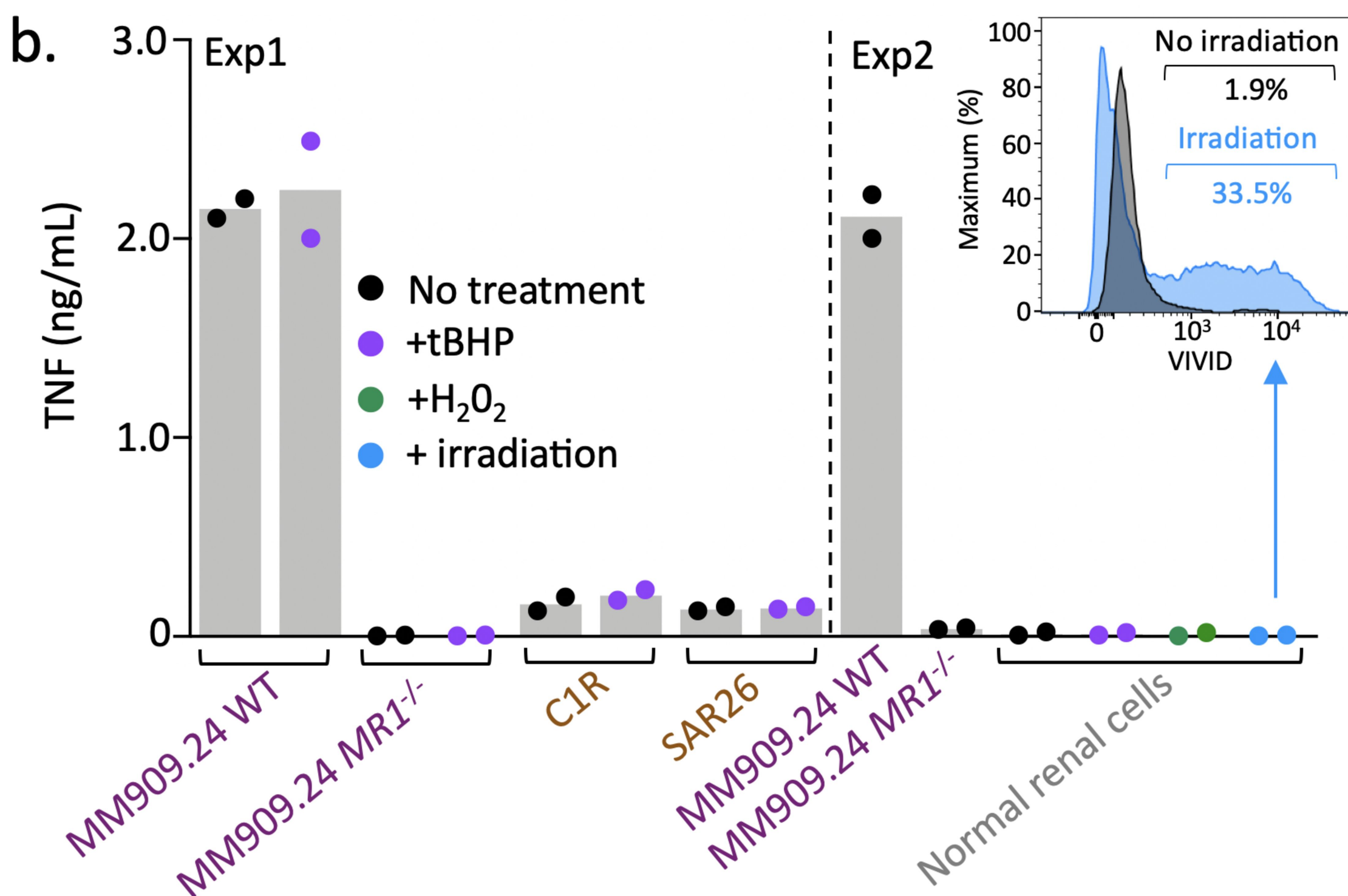
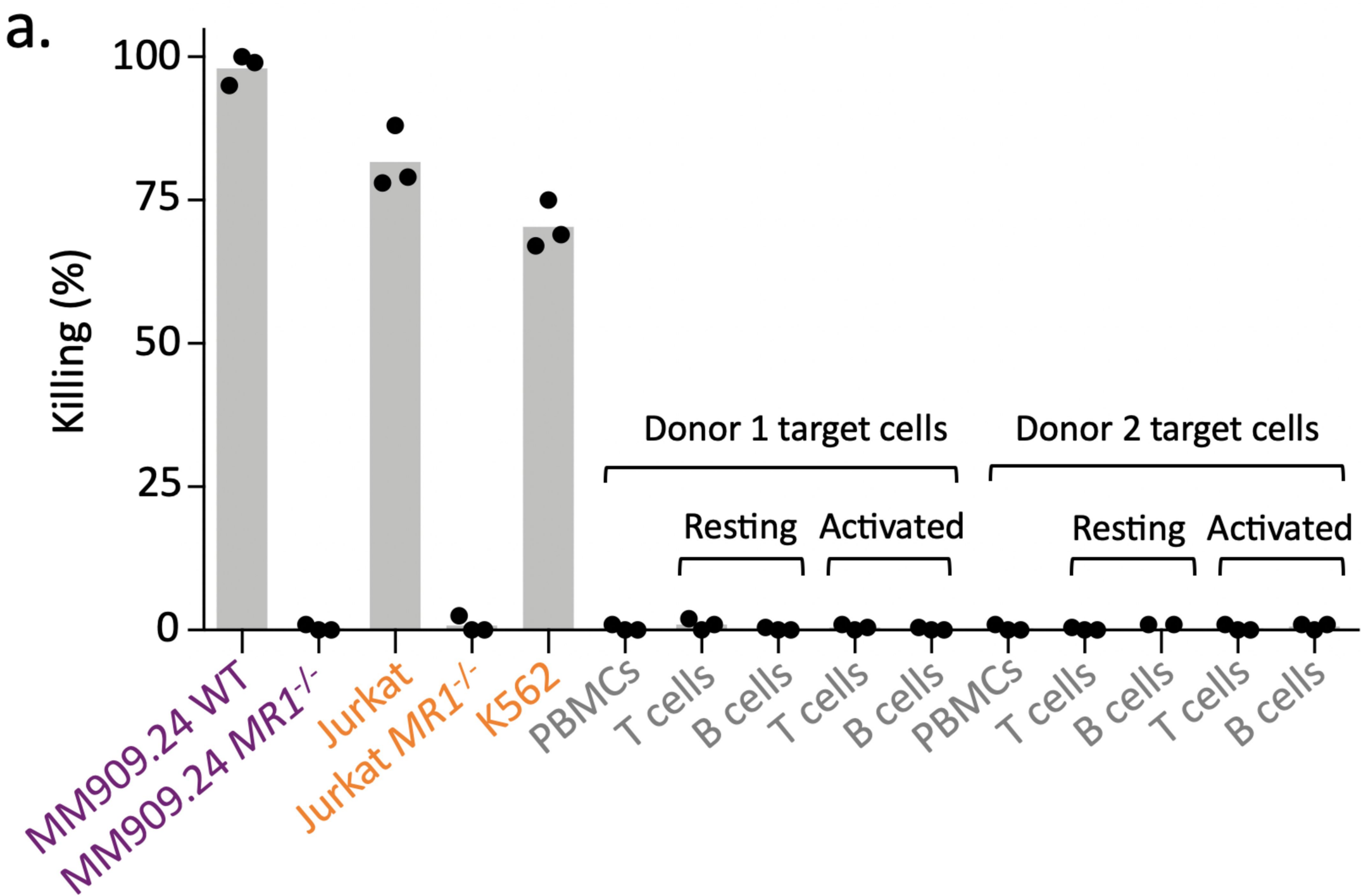






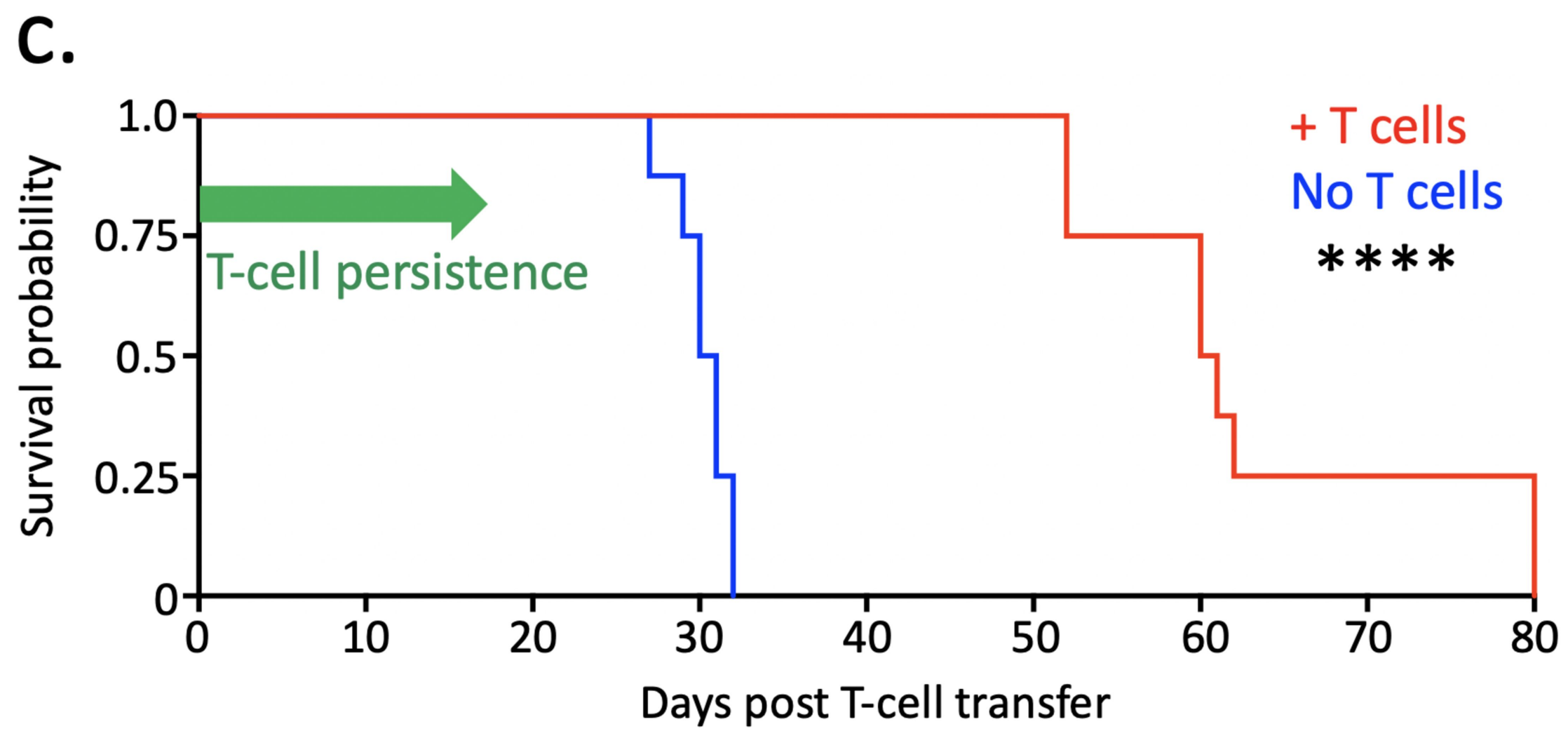
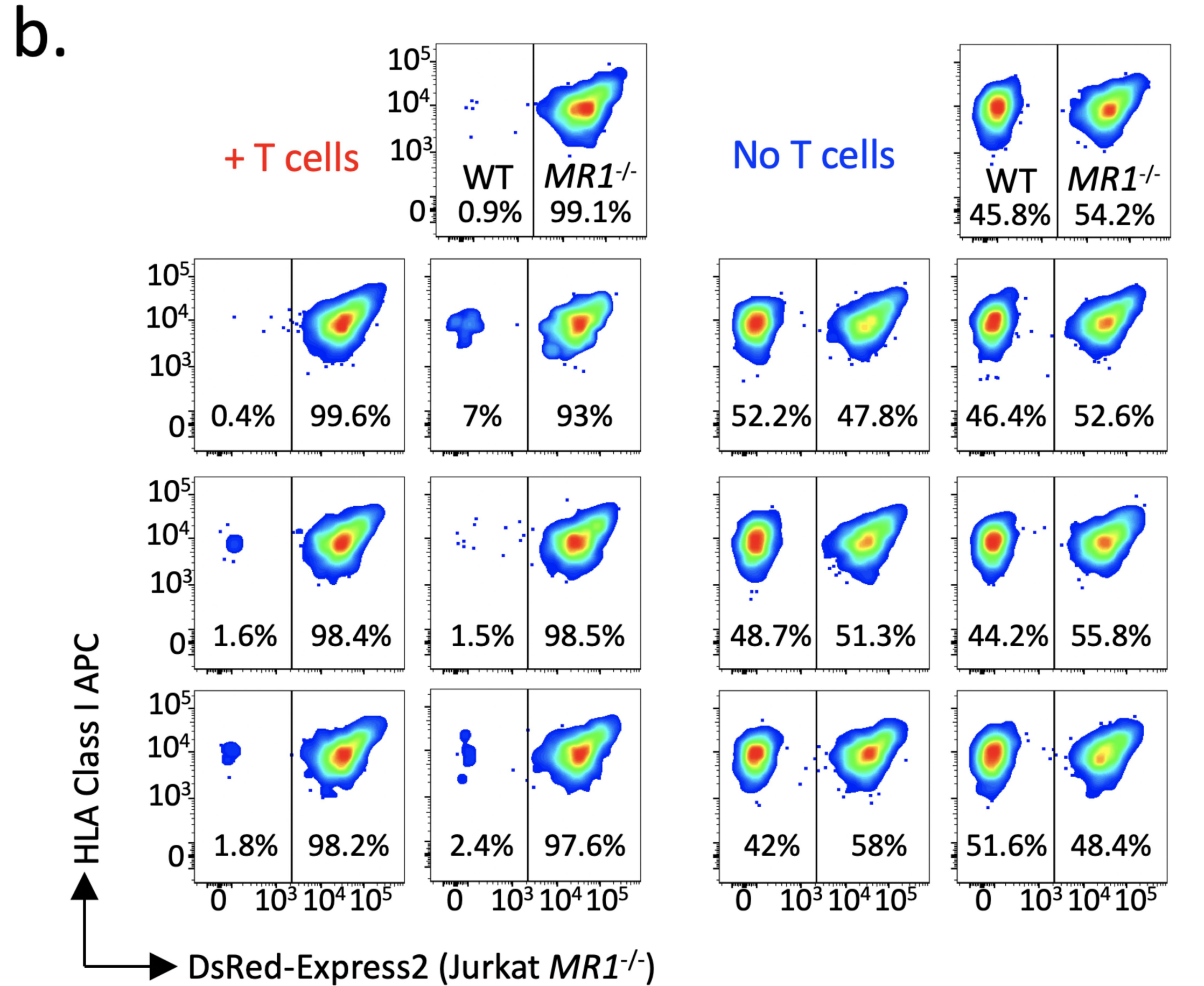
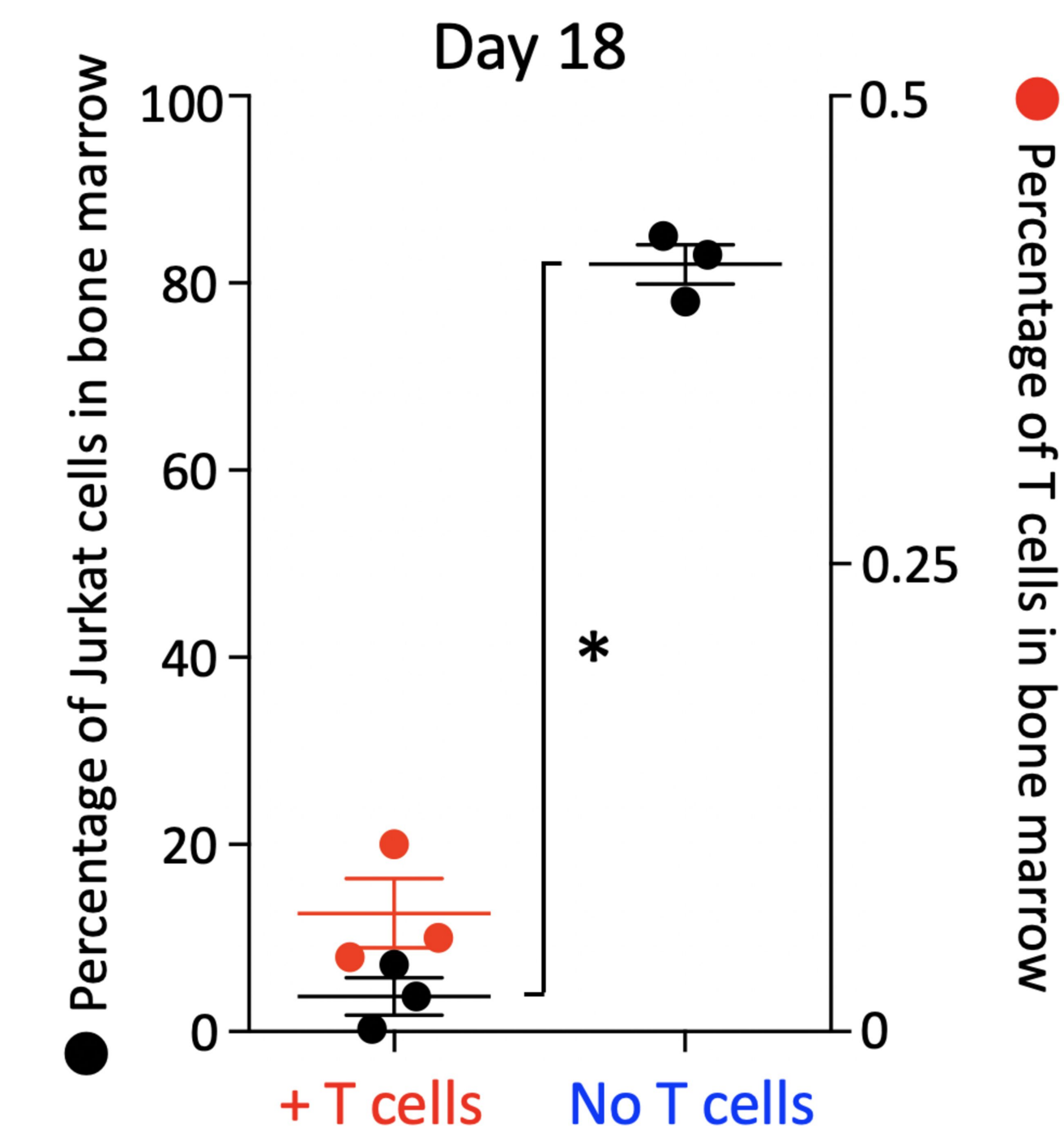
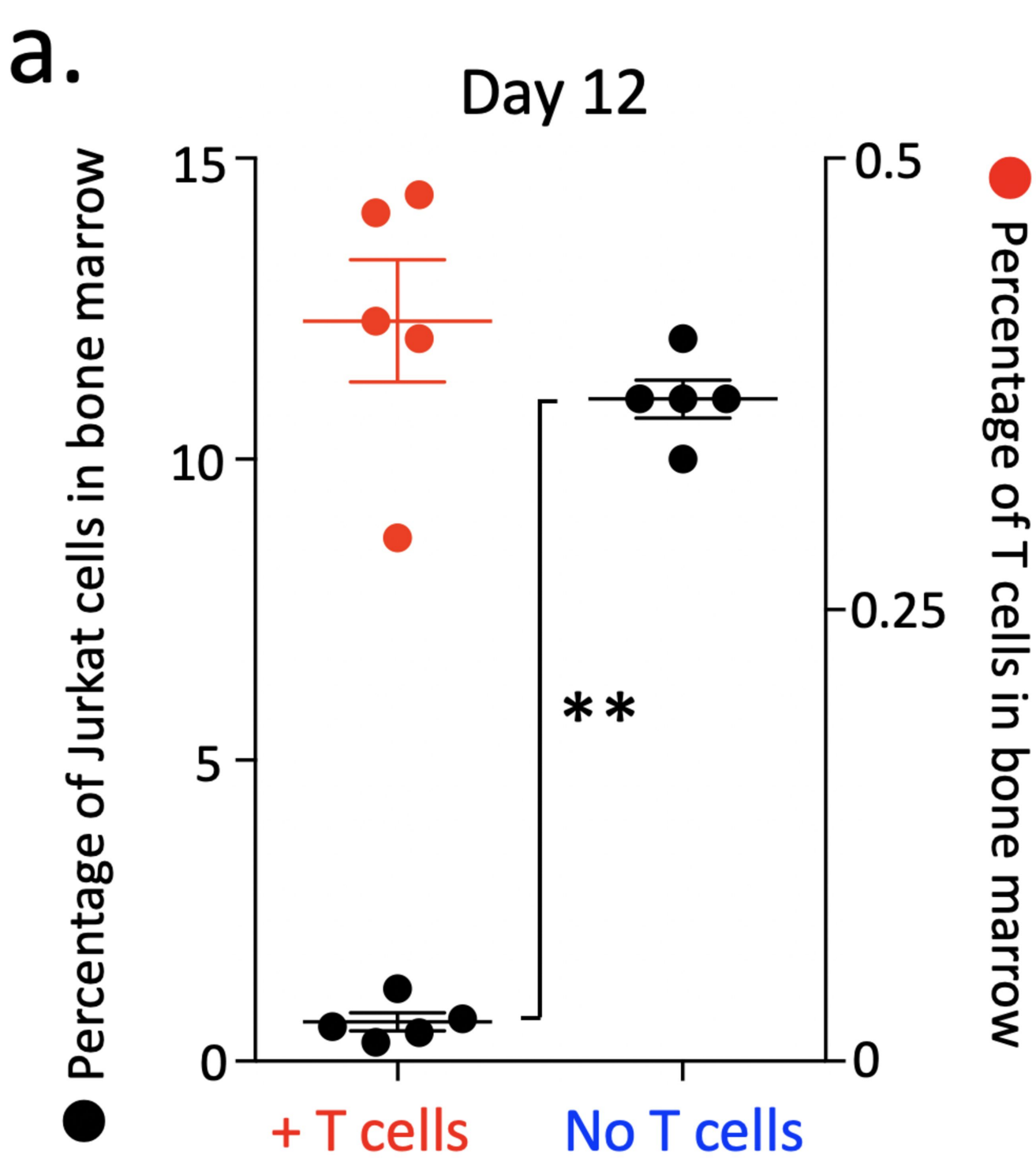






Key: Lung cancer Melanoma Leukaemia Normal/healthy cells Lymphoblastoid cell lines

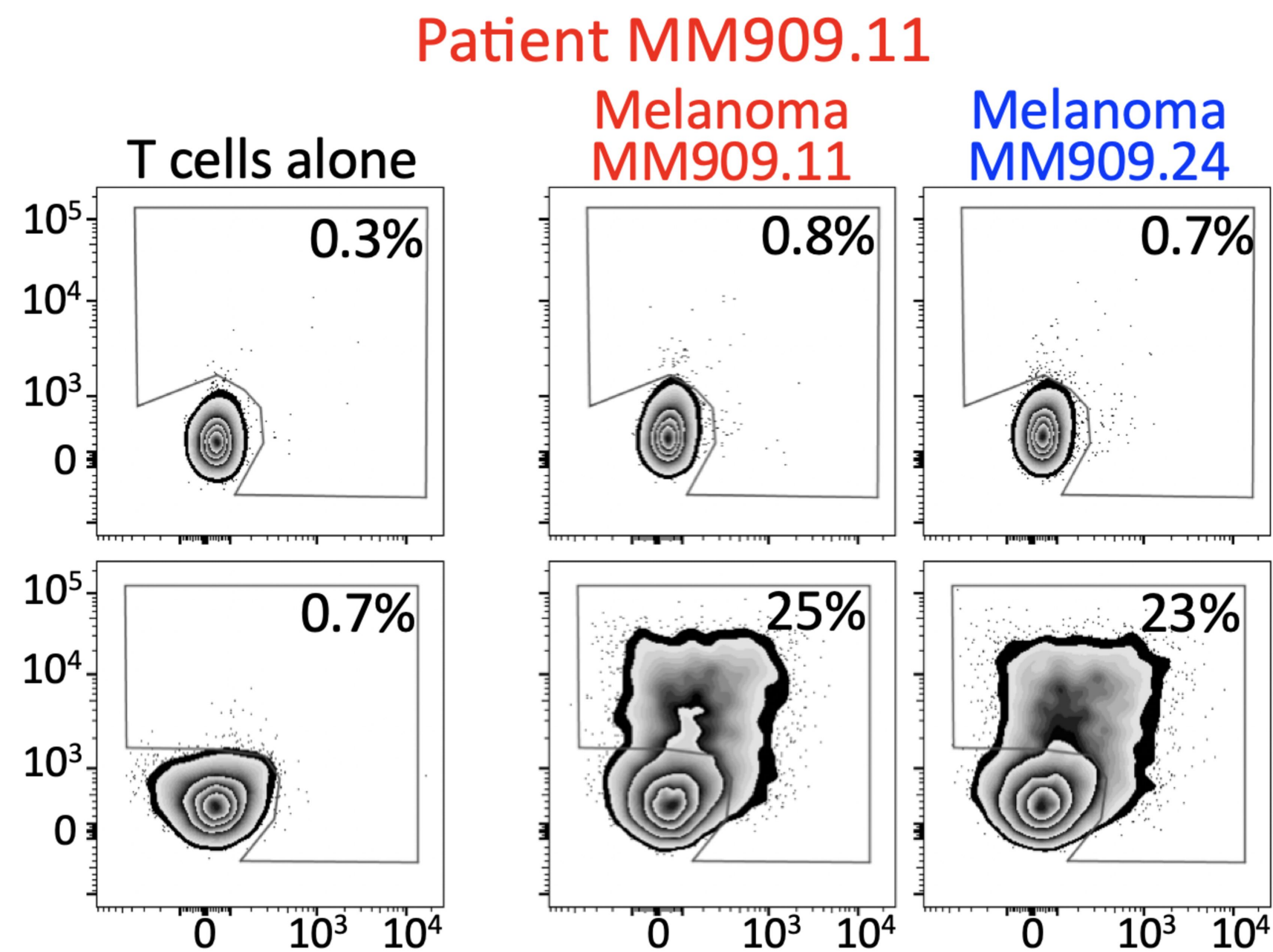






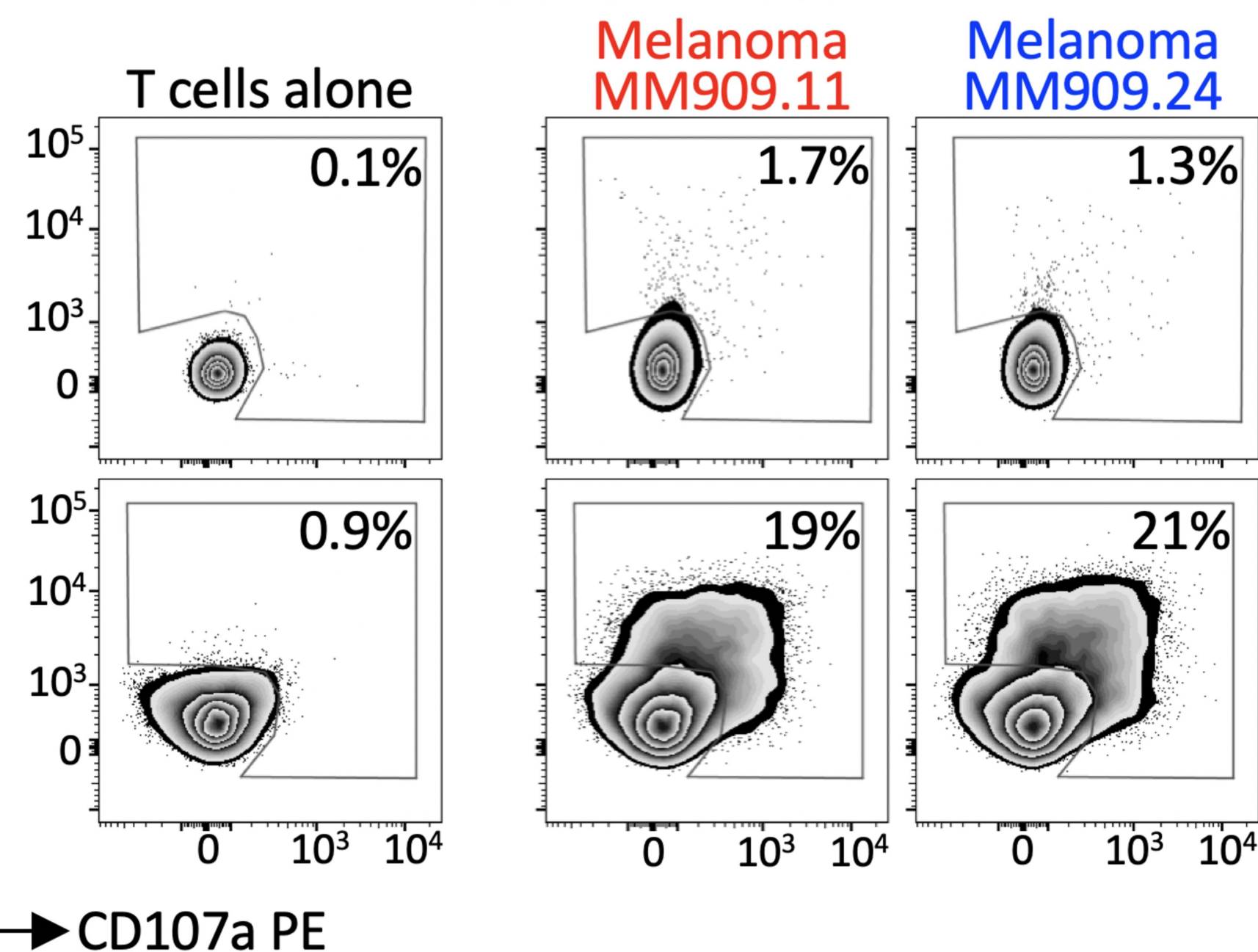
a.

+ MC.7.G5 TCR    No TCR

**Patient MM909.24**

+ MC.7.G5 TCR    No TCR

TNF PE-Vio770



b.

Melanomas

